Spectral Analysis for Rod Formation Dynamics

by

Shannon Thomas Stewart

Thesis submitted to the Faculty of the

Virginia Polytechnic Institute and State University

in partial fulfillment of the requirements for the degree of

MASTER OF SCIENCE

in

Mechanical Engineering

APPROVED:

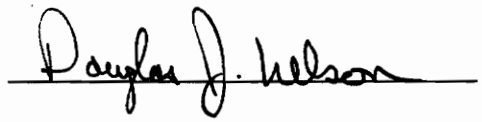

Dr. Douglas J. Nelson, Chairman

Dr. Charles F. Reinholtz

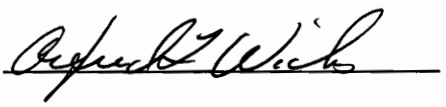

Dr. Alfred L. Wicks

April 26, 1995

Key words: Signal Processing, FFT, Rod Production, Fourier

c.2

Spectral Analysis for Rod Formation Dynamics

by
Shannon Thomas Stewart
Dr. Douglas J. Nelson, Chairman
Mechanical Engineering

(ABSTRACT)

This thesis deals with the production of a continuous rod of non-uniform properties which is formed by wrapping fibers with a thin membrane. This rod is driven axially and cut into segments. Measurements of pressure, temperature, axial force, axial velocity, horizontal and vertical displacements were taken of the rod during normal operating conditions at various speeds. The time signal for these tests were converted to the frequency domain through the use of a Fast Fourier Transform (FFT). The data was then examined to determine the inputs into the rod from various components of the rod producing machine.

The results of the experiments show that the machine has inputs in several location along the production line. It also shows that changing components of the machine based on their frequency response may be beneficial in minimizing the number of stoppages in the production of the rod. This investigation into the dynamics of rod production shows that there is a potential for significant gains in production by altering certain components of the production machines. This report also offers a future test procedure that should help to better explain the rod's motion and thus may lead to more efficient production.

ACKNOWLEDGMENTS

I would first like to thank Dr. Douglas J. Nelson, my advisor, for allowing me the opportunity to participate in this project and for giving me a chance to attend graduate school. I would also like to thank him for the advice he has given me about other ventures that I have been debating.

To the members of my graduate committee, Dr. Charles F. Reinholtz and Dr. Alfred L. Wicks, thank you for the advice during this project.

I would like to thank Eddie Williams who helped me adjust to graduate school. Also Eric Johnstone, Brian Nutter , and Kevin Riutort who also worked on this project.

To my family, Tom, Arvella, Morgan, and Amber who have always encouraged me in everything that I have done. Also my grandparents Bonnie Berry, Edith and Eugene Stewart who have given me advice that can not be replaced.

Last, but not least, Michelle Bishop who has been at my side during this long stay at Virginia Tech. Thank You All.

TABLE OF CONTENTS

LIST OF FIGURES

LIST OF TABLES

NOMENCLATURE

$a_o, a_1, a_2, \ldots a_k$	-	coefficients of Fourier series
$b_o, b_1, b_2, \ldots b_k$	-	coefficients of Fourier series
$e^{i\omega t}$	-	$\cos(\omega t) + i\sin(\omega t)$
f_o	-	minimum collection frequency
i	-	$\sqrt{-1}$.
k	-	variable integer
t	-	time
$x(t)$	-	arbitrary function in time
$E[\ ]$	-	ensemble averaged value of quanity in the brackets
N	-	number of collected data points
$R()$	-	correlation function
$R_{xy}(), R_{yx}()$	-	cross-correlation function between x(t) and y(t)
T	-	period of an arbitrary function in time
		GREEK SYMBOLS
ρ	-	correlation coefficient
τ	-	time lag
π	-	$\cos^{-1}(-1)$
ω	-	angular frequency
Δ	-	sampling interval

I. INTRODUCTION

Note: Since some of the material discussed in this thesis is of a proprietary nature, care has been taken to word things as generally as possible.

General Background

A continuous rod of non-uniform properties can be formed by wrapping fibers with a thin membrane. Figure 1.1 illustrates the entry region of this process.

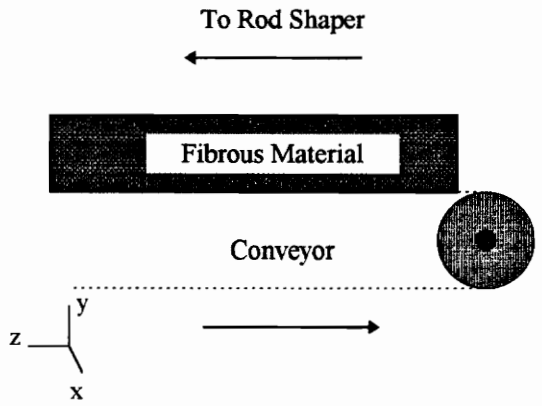

Figure 1.1: Side View of Conveyor and Material

The fibrous material is placed on a moving flexible conveyor. When the material is placed on the conveyor it is in the form of a cake, which has a cross-sectional aspect ratio of approximately one. From this point the material is carried into a rod forming device, where the cake's cross-sectional shape is converted from a square into a circular shape. At this stage in the process the rod shaper causes the flexible conveyor and thin membrane to envelop the fibrous material. The membrane encompasses the material, except for one

region on the top of the rod, which is left open to be sealed after the shaping process. Figure 1.2 illustrates this region on the rod. The next stage in the process is the sealing process which overlaps the membrane onto itself and seals this overlap with adhesive. From this point in the process, the rod is moved through an open region where it is supported by a rod support. From here, it continues on to the cutter where it is cut into segments. This is the final stage in the process.

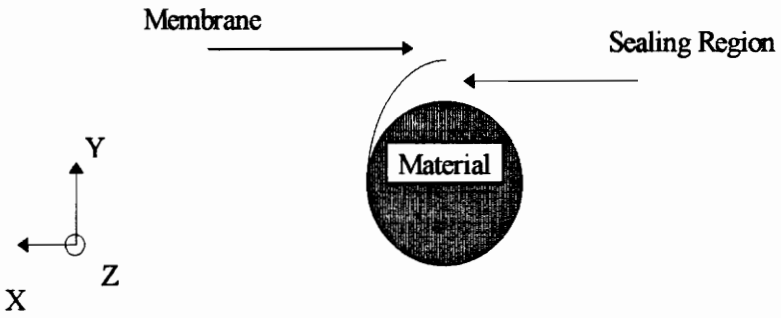

Figure 1.2: End View of Rod To Show Sealing Region

The rod is affected by many operating parameters. The machine inputs forces onto the rod in several different locations during operation. These inputs include the rod shaper, the conveyor belt, the rod support, the cutter, and of course the regular operating vibrations of the machine. The dynamics of the rod are directly related to all the inputs from the machine. The resulting response of the rod has both the characteristics of the rod's response and the machine's operating vibrations. The operating vibrations of the

machine can be seen in the frequency spectrum of the rod's response. An overall view of the process is shown in Figure 1.3.

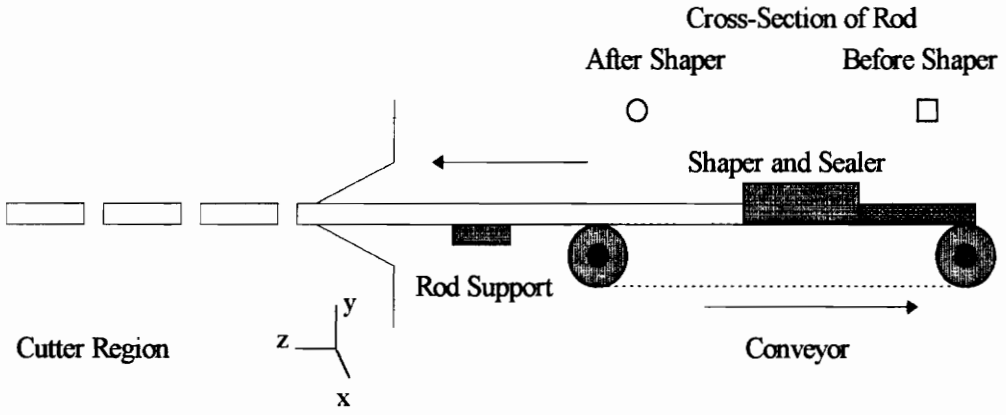

Figure 1.3: Schematic of Overall Rod Production Process

The motion of the rod must be limited due to the fact that too much motion in the rod will lead to its failure, which is an actual breakage of the rod. A failure of the rod causes stoppage in its production.

Objectives

The objectives of this research are two fold. The first is to improve the overall rod production process. An improvement in the rod production would be a decrease in the number of breaks of the rod, and thus fewer production stoppages. To perform the first objective, a second objective is required: identify the various inputs on the rod and describe the motion of the rod. If the inputs to the rod could be identified, then failures in the process could be better explained and thus possibly resolved. The motion of the rod could also lend a clue as to the behavior of the rod failures.

In order to resolve the inputs and to describe the motion of the rod, testing for several operating conditions were required. These tests included conditions for various operating speeds and two materials, A and B. Also one component of the machine, the rod supporter, was changed during testing to evaluate the effect it had on the rod. The rod supporter is shown in Figure 1.4.

Methodology

This section gives background to some of the main processes and mathematical procedures needed in this work. The main areas covered by this survey are 1) general rules to follow for digital data collection, 2) Fourier's series expansion to acquire individual frequencies from a large spectrum of frequencies, 3) the Fast Fourier Transform (FFT) for converting a time domain signal into the frequency domain, and 4) averaging for statistically sound data interpretation .

Digital Signal Collection

Computers are becoming more powerful everyday. This has allowed digital signal collection to become an increasingly useful tool for data collection. The sample rates allowed by this method have reached into the megahertz range. There are various methods employed by engineers and technicians to collect and evaluate data, but there are general rules that are commonly followed. These rules are used to improve the validity of the data collected.

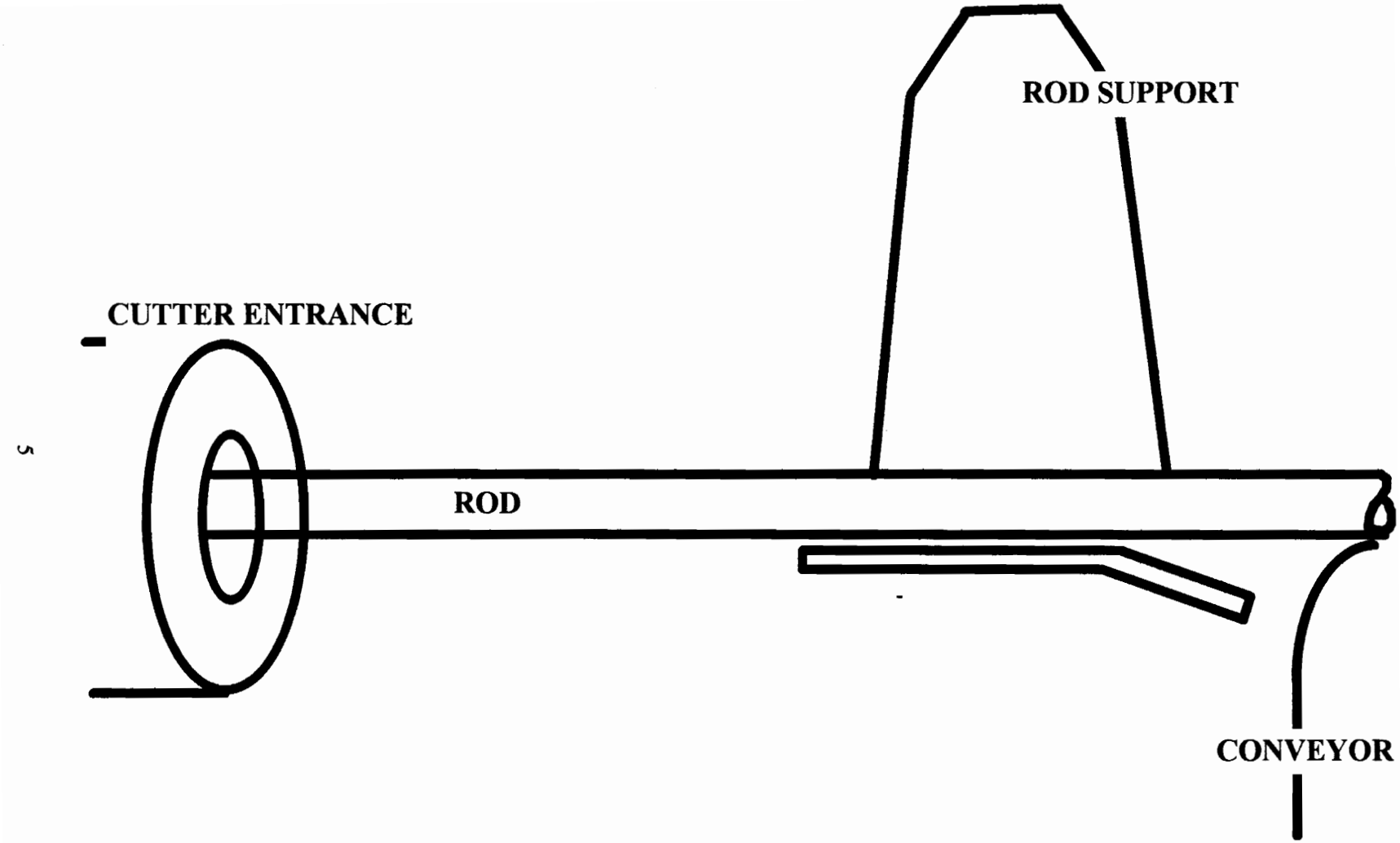

Figure 1.4: Rod Support Region

The first is how to estimate the minimum frequency that can be attained during testing. This is hardware dependent, but follows a simple equation.

$$f_o(\text{Hz.}) = \frac{1}{N\Delta t}$$

The equation states the smallest frequency that can be resolved (f_o) is equal to one divided by the quantity of the number of points taken(N) times the time step size of the process. Therefore to resolve a low frequency, which in the time domain has a long period, the collection of data must be for an extended period of time, i.e. N must become large.

The second point of interest is the maximum frequency that can be resolved. As Δt decreases, the number of points taken in a given time interval increases. This means that changes (frequencies) in the time interval will be caught in the data since more points are now taken in that time interval.

The third idea needed for the basic understanding of general digital data collection is aliasing. Aliasing is the mathematical problem that occurs when dealing with finite length discrete data. The true spectrum that would come from an infinite series does not match exactly with the calculated spectrum from a discrete Fourier transform (DFT) after a frequency that is greater than one half of Δt^{-1}. After this spectral line, the spectrum begins to fold back onto itself, thus corrupting the frequencies below $\frac{1}{2}\Delta t^{-1}$. This frequency is known as the Nyquist frequency or is sometimes called the folding frequency.

In the end, clear goals must be set to determine the minimum and maximum frequencies that need to be gathered. To resolve both a low frequency and a high frequency, a large N must be used and a small Δt must be used. In hardware concerns this means money, due to the fact that a large N will require more data storage and a small Δt will require faster data collection units.

Fourier's Series Expansion

The Fourier series is a widely used mathematical approach for representing a periodic function of period T in terms of an infinite series of orthogonal trigonometric functions. These trigonometric functions are commonly sines and cosines. Therefore the general function in Figure 1.5 can be expressed by:

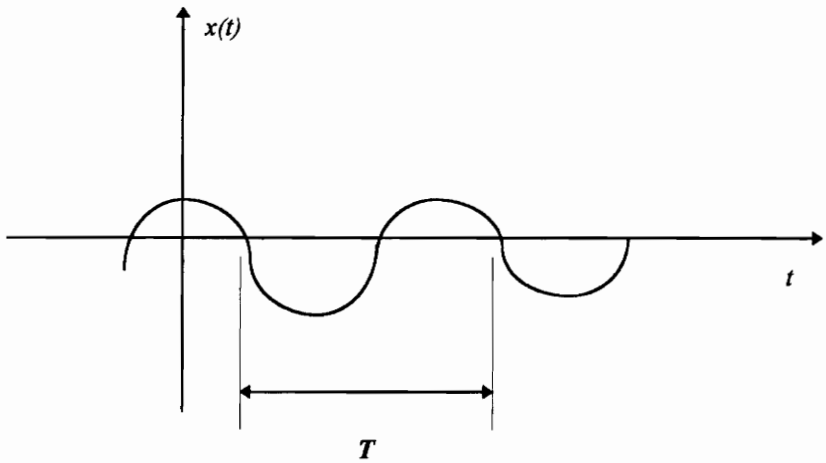

Figure 1.5: Arbitrary Periodic Function in Time

$$x(t) = a_o + a_1 \cos\left(\frac{2\pi t}{T}\right) + a_2 \cos\left(\frac{4\pi t}{T}\right) + \ldots$$

$$b_1 \sin\left(\frac{2\pi t}{T}\right) + b_2 \sin\left(\frac{4\pi t}{T}\right) + \ldots$$

This equation can be expressed in a more compact form:

$$x(t) = a_o + \sum_{k=1}^{\infty}\left(a_k \cos\left(\frac{2\pi kt}{T}\right) + b_k \sin\left(\frac{2\pi kt}{T}\right)\right)$$

where a_o, a_k, and b_k are constant Fourier coefficients given by:

$$a_o = \frac{1}{T}\int_{-T/2}^{T/2} x(t)dt$$

a_o is the mean of the given function.

$$a_{\substack{k \\ k\geq 1}} = \frac{2}{T}\int_{-T/2}^{T/2} x(t)\cos\left(\frac{2\pi kt}{T}\right)dt$$

$$b_{\substack{k \\ k\geq 1}} = \frac{2}{T}\int_{-T/2}^{T/2} x(t)\sin\left(\frac{2\pi kt}{T}\right)dt$$

These constants represent the harmonics of the spectrum. The function that was originally given in time can now be expressed in the frequency domain as shown in Figure 1.6.

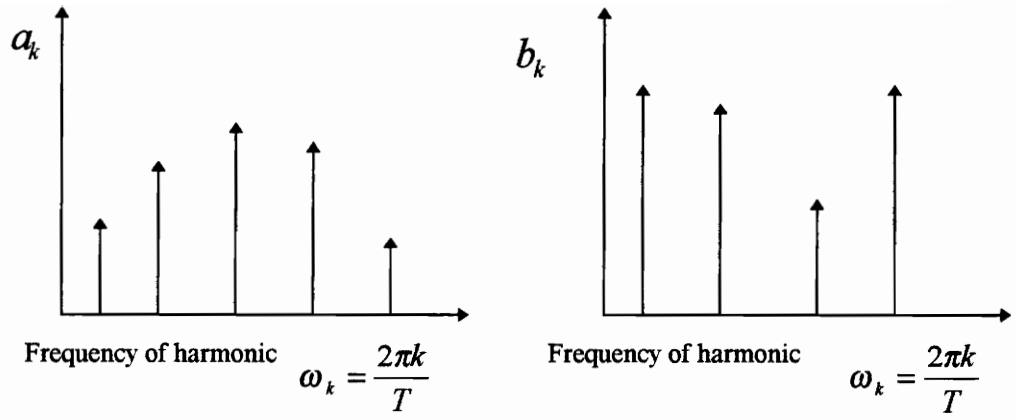

Figure 1.6: Graphical Representation of Fourier Coeffients

Where the spacing between the spectral lines is $\Delta\omega = \frac{2\pi}{T}$.

Fast Fourier Transform

The practical use of the Fourier expansion is a discrete form that can easily be programmed into a computer, which can automate this tedious mathematical procedure. As in most discrete applications of continuous mathematical expressions, the integrals are replaced with a summation over a given range of numbers. This range is set by the number of data points collected. Using an altered form of the equations given in the previous section, it can be shown that

$$x(t) = a_o + 2\sum_{k=1}^{\infty}\left(a_k \cos\left(\frac{2\pi kt}{T}\right) + b_k \sin\left(\frac{2\pi kt}{T}\right)\right)$$

where

$$a_{\substack{k\\k\geq 1}} = \frac{1}{T}\int_0^T x(t)\cos\left(\frac{2\pi kt}{T}\right)dt$$

$$b_{\substack{k\\k\geq 1}} = \frac{1}{T}\int_0^T x(t)\sin\left(\frac{2\pi kt}{T}\right)dt$$

can be converted into a single equation by combining the following terms:

defining $X_k = a_k - ib_k$

setting $e^{-i(2\pi kt/T)} = \cos\left(\frac{2\pi kt}{T}\right) - i\sin\left(\frac{2\pi kt}{T}\right)$

yields $$X_{\substack{k\\k\geq 0}} = \frac{1}{T}\int_0^T x(t)e^{-i(2\pi kt/T}dt$$

From this equation, if x(t) is assumed to be discrete the following equation applies:

$$X_k = \frac{1}{N}\sum_{r=0}^{N-1} x_r e^{i(2\pi kr/N)}$$

Where r is the value of time divided by a step delta. This equation yields both real and imaginary components. The real components represent the amplitude information from the data; whereas, the imaginary components reveal the phase information about the data.

Averaging

Averaging is the process of taking several sets of data, summing them, and then dividing by the number summed. This acts to improve the statistical validity of the information. When using more than one data set, the flaws or abnormalities in the data are distributed, thus lowering the chances of one abnormality in the data leading to the incorrect interpretation of the data. Data can be averaged in more than one way. One approach is to actually numerically average the data. Another approach is to evaluate several tests visually. If the data in all the tests are close or nearly the same, then the data is well behaved and the use of numerical averaging may not be as useful.

The calculation of averages is fairly straight forward process. Consider the mean value of x which is represented by E[x] where the E stands for "the statistical expectation of". With mean value of the time history of x over an interval T calculated the ensemble average is defined to be $E[x] = \int_0^T x(t)\frac{dt}{T}$.

II. TEST PROCEDURE

Test Setup

The procedure followed for these experiments evolved from one test to the next. Each test gave clues to the behavior of the rod, but also left questions to be answered about the rod motion.

First Test

The first set of tests were conducted by using high speed video equipment to record the motion of the rod during normal operation. The video camera used 2000 frames/sec. This was an attempt to visually inspect the rod during operation and try to identify the shape of the rod before and during failure. The high speed video camera was set up as illustrated in the schematic in Figure 2.1.

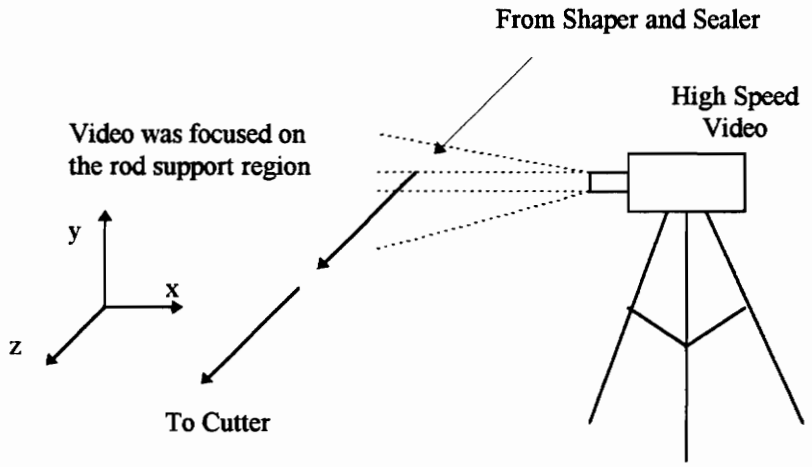

Figure 2.1: High Speed Video Placement

These video tests showed that the rod movement had larger displacements during normal operating conditions than had been previously thought. Also observed from these video tests was a frequency that could be seen in the vertical movement of the rod. This information led to the need for further testing. One goal of another test was to identify the frequency gained from the visual inspection and to pinpoint its source.

Second Test

The second series of tests was developed to collect actual real time numerical values for the vertical displacement of the rod. By collecting data at a fast enough rate, it was thought that machine frequencies could be seen in the data. Also of interest was the axial shear force, the temperature, and the pressure effects that the rod shaper had on the rod. Two other components in the testing were a rod break signal and segment pulse signal, which are both built into the machine for stoppage after failure of the rod and alignment of the timing of the machine. By using the rod break signal as a trigger, it could be determined where and when in the data that the actual failure occurred. Also the segment pulse signal allowed the data to be aligned with the frequency of the cutter and other processes in the production. The displacement measurements were accomplished by the use of a laser displacement device. This laser was mounted as shown in Figure 2.2.

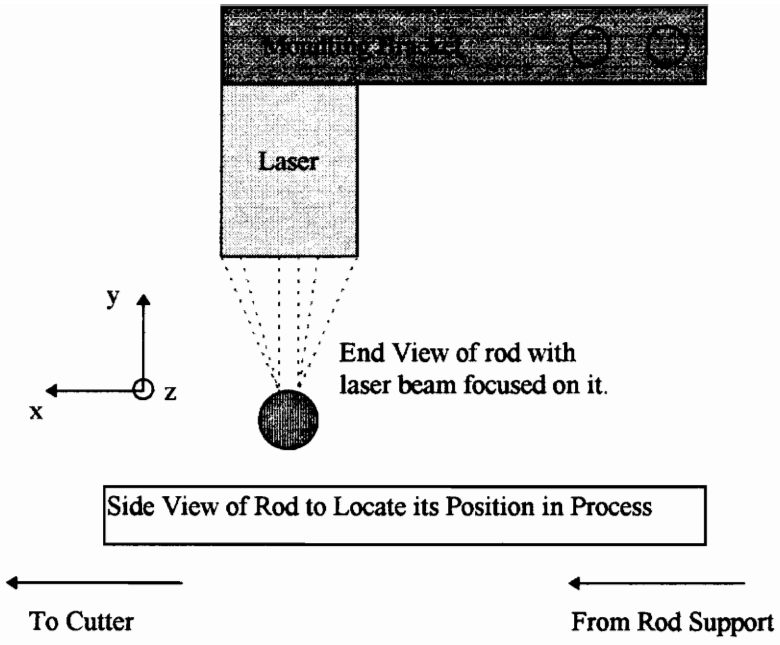

Figure 2.2: Displacement Laser Placement

The pressure measurements were accomplished by placing a pressure tap in the rod shaper. The pressure tap was a constant flow device that forced a constant flow of air through a tube that led to the pressure tap hole in the rod shaper. The idea behind the mechanism was that changes in the pressure in the rod shaper, due to the axial velocity of the rod, would cause a change in the air flow in the tube. The mechanism would work to maintain the constant flow rate, thus the changes need to maintain the constant flow could be measured and related to the pressure change in the rod shaper. This is illustrated in Figure 2.3. The axial shear component was measured by placing the rod shaper on two vertical pins that limited the shaper to only vertical movements. With this in place, a strain gauge was mounted in the shaper in the direction of axial motion. By allowing vertical movement only, it was believed that the axial force of the rod could be measured. This is

also shown in Figure 2.3. The temperature was measured by placing a thermo-couple in the shaper and measuring its output, also Figure 2.3.

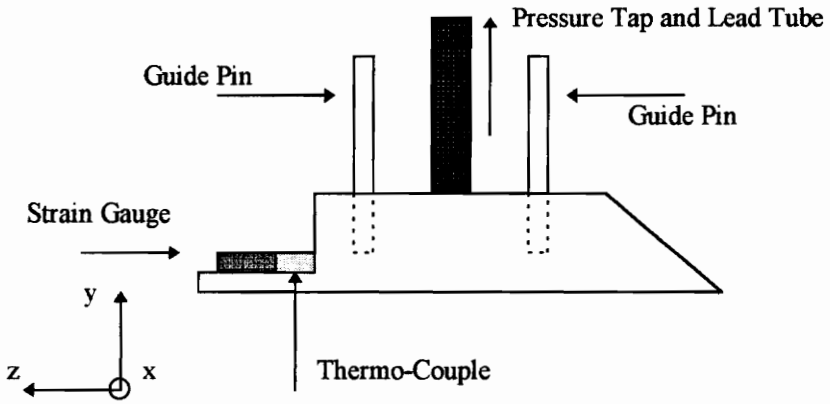

Figure 2.3: Side View of Rod Shaper With Test Equipment

The last component in this array of tests was the use of a Doppler laser to measure the axial velocity of the rod. The details of the hardware components for this set of tests are given in Table 2.1. This table contains three headings. The first heading is the description of the test component used in this array. The second is the frequency response of the module used. The third is the status of the component during the actual testing. The status column has three descriptions. A status of 'On-line and Recorded' means the data was collected and stored to disk. While testing, it was seen that this component was not responding adequately and will be discussed in a later section. 'On-line and Observed' means the component was not recorded to disk, but was visually inspected from time to time during testing.

Table 2.1: Test II. Components and Responses

Test Module	Sample Rate	Status
Strain Gauge Module	10 kHz.	On-line and Recorded
Y-Axis Displacement Laser	10 kHz.	On-line and Recorded
Laser Doppler (Velocity)	10 Hz.	On-line and Recorded
Draft Pressure	10 kHz.	On-line and Recorded
Rod Break	10 kHz.	On-line and Recorded
Segment Pulse	10 kHz.	On-line and Recorded
Temperature	10 kHz.	Off-line and Observed

After this series of tests was concluded, it was found that it would be beneficial to have another series of tests.

Third Test

In the third array of testing it was thought that having horizontal movement of the rod incorporated in the tests could help better explain the motion of the rod. The pressure, velocity, and temperature measurements were taken in the rod shaper again, but this time the axial force measurements were not. The reason will be explained later in this text. The x-axis measurement was added at the same location as the y-axis displacement. The bracket that was designed to hold the y-axis laser was redesigned to accommodate the x-axis laser, as shown in Figure 2.4. Table 2.2 illustrates the hardware and its status for these sets of tests.

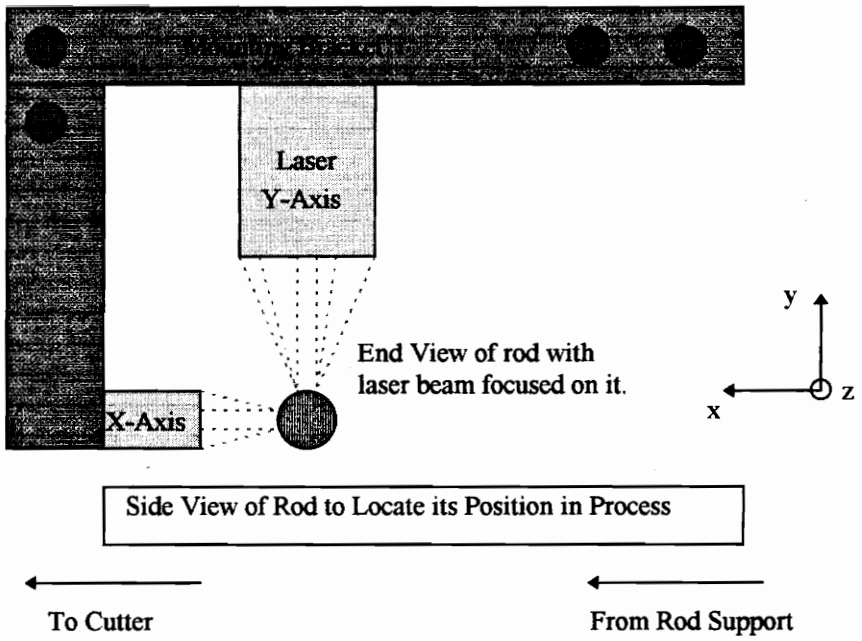

Figure 2.4: Displacement (X and Y) Laser Placement

Table 2.2: Test III Components and Responses

Test Module	Sample Rate	Status
Draft Pressure	10 kHz.	On-line and Recorded
Y-axis Laser Displacement	10 kHz.	On-line and Recorded
Laser Doppler (Velocity)	10 kHz.	On-line and Recorded
X-axis Laser Displacement	10 kHz.	On-line and Recorded
Rod Break	10 kHz.	On-line and Recorded
Segment Pulse	10 kHz.	On-line and Recorded
Temperature	10 kHz.	On-line and Recorded

III. DATA EVALUATION

Test Set One

As mentioned previously, the first set of tests were a visual investigation of the rod's motion by using a high speed video camera. The tape from the camera was played back frame-by-frame to try to identify any motion in the rod that might occur during normal operation or during the moments just before failure of the rod. From the film, it was apparent that the rod did have a motion to it that could not be seen by the naked eye. The rod oscillated in the vertical direction at approximately 60 Hz. This frequency would normally throw a red flag in the evaluation of the data, since the electrical line frequency is in this range. In this case however, the data was visual and it had been collected at 2000 frames/sec. The 60 Hz. frequency also corresponded to the operating frequency of the cutter at 8000 rods/min. Since the cutter is a drum that has two blades, the cutter frequency is 66.67 Hz. The video tests confirmed that the inputs from the cutter were propagating upstream in the rod. By identifying that this did occur, it was believed that further testing would lead to a more concrete understanding of what components had inputs and what the magnitude of these components were.

Test Set Two

The second array of tests were designed to retrieve data that would give actual numerical values for the magnitude of the inputs on the rod. From this data, it was

believed that the rod's reaction to the inputs could be determined and explained. It should be noted at this point, unless otherwise stated, that the data shown and manipulated is mean zero. Mean zero data refers to data that has had the average value removed, which is the same as removing the DC offset. As with many initial experiments, the data retrieved is later found to be erroneous, as was the case in certain components of this test array. Each component of this test will be discussed and an explanation of the error in the data will be explained where appropriate.

Machine Speeds

In this array of tests, the operating speeds of the machine were varied. The machine was made to run at two speeds, 8000 units/min. and 5000 units/min. Also, during the course of testing, the rod was tampered with to induce failure in an attempt to determine characteristic patterns in frequency spectrum for certain failure modes. However, this proved useless due to the fact that as soon as the perturbation was introduced failure occurred and then after failure the signal was completely random. Meaning the data recovered after the induced perturbation was not periodic and thus a DFT will not work. Thus the data after this point was truncated.

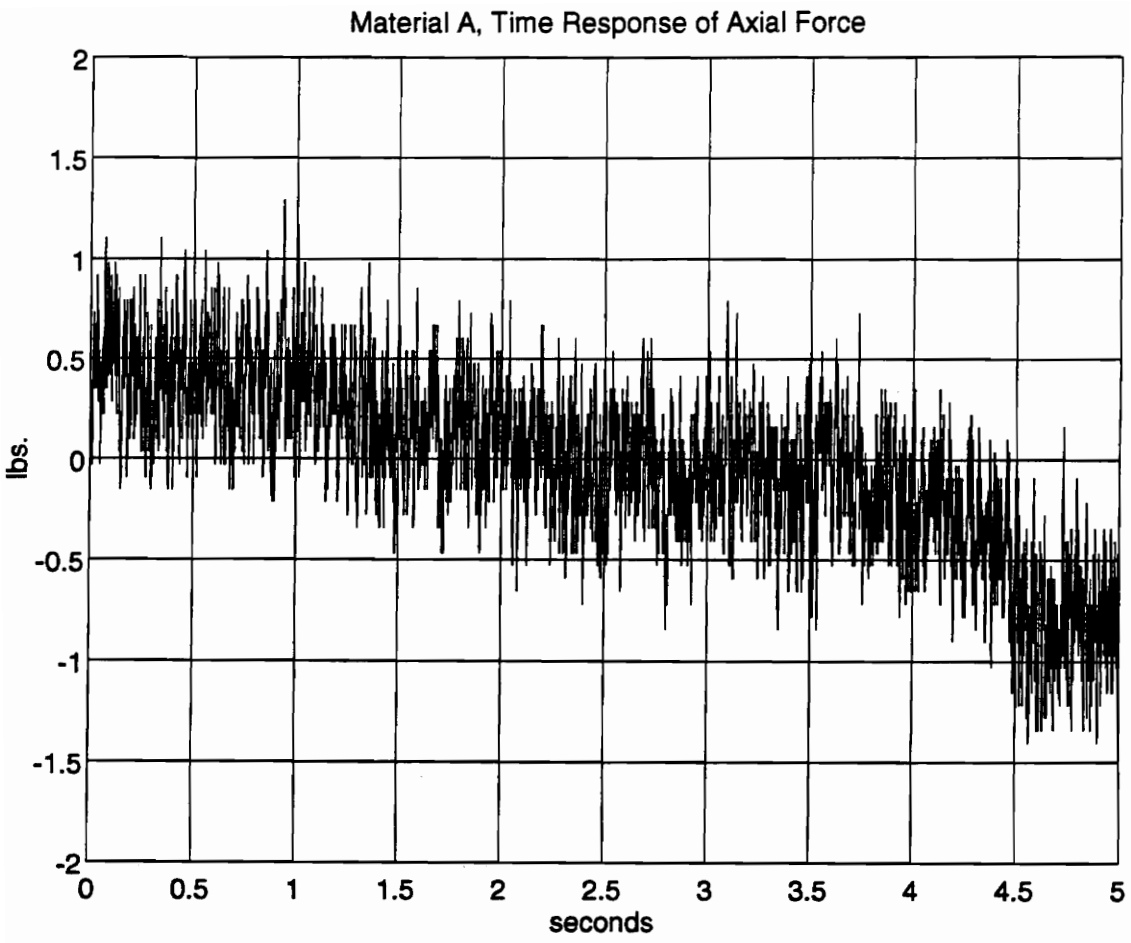

Note: This is a plot of the time signal from the data collected from the attempted force measurement. This was placed in the report to illustrate that the data from this measurement is not stationary.

Figure 3.1: Time Response of the Strain Gauge

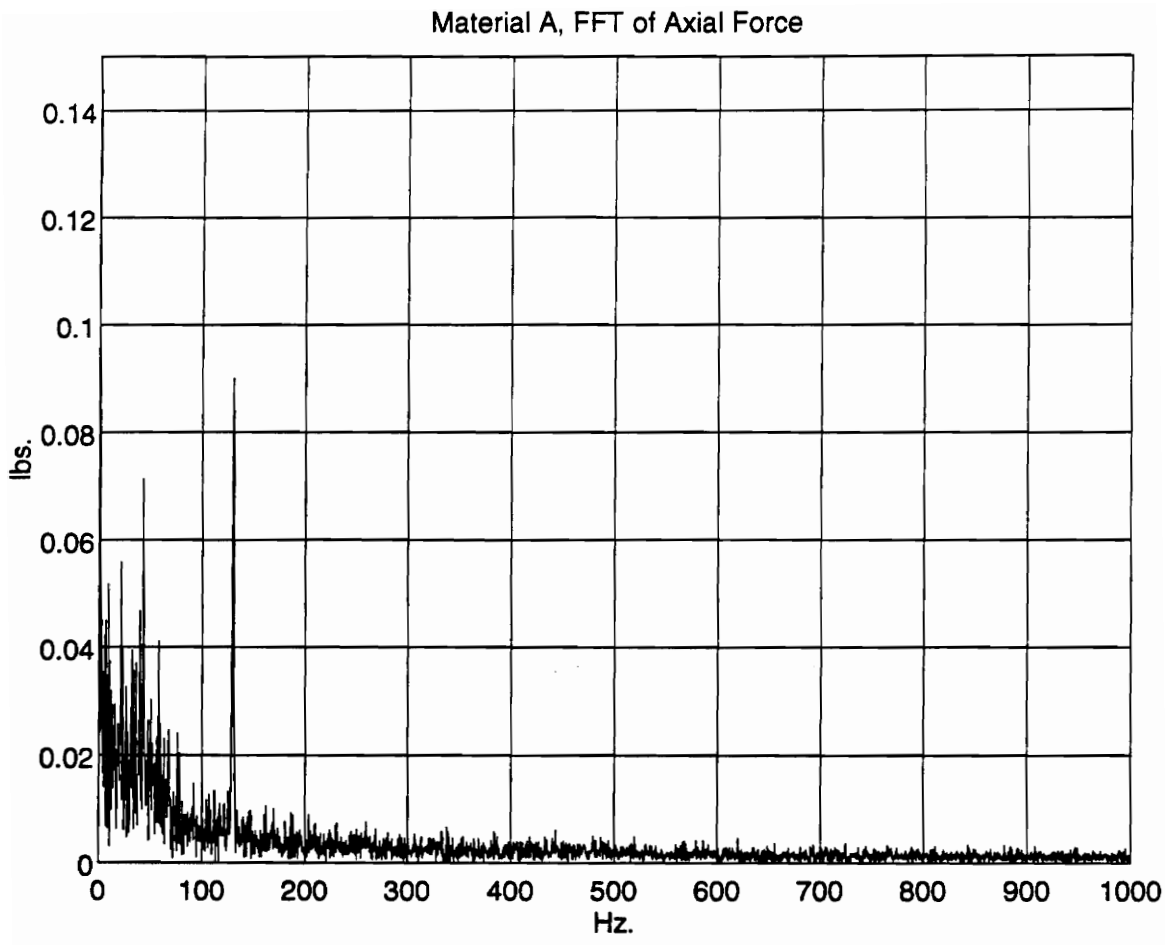

Note: This is a plot of the frequency spectrum from the data collected from the attempted force measurement. This was placed in the report to illustrate that the data from this measurement is not stationary.

Figure 3.2: FFT of the Strain Gauge Measurements

Axial Force Measurement

The retrieved data from the strain gauge was not valid for this application. The point of this experiment was to determine the frequencies of the inputs on the rod shaper that propagated upstream from other components in the machine. The equipment used had a fast enough response time to accomplish this task; however, the actual rod shaper did not lend itself well for this measurement. It was assumed before the testing that the input from downstream on the rod shaper would be small, and this was proven in the response of the strain gauge. The rod shaper itself acted as a damper to eliminate the inputs. The time response of the signal gained from the strain gauge is shown in Figure 3.1. One thing to notice is how the mean zero data trails off. This means that the data is not stationary or in other words is not steady. Since the data is not stationary, the FFT shown in Figure 3.2 is not valid. This data looks as though some components in the test rig were not set properly and were moving or vibrating during operation. Another cause could be that the machine did not run long enough to attain a real steady-state value.

Y-Axis Laser Displacement

The results from the laser data proved much more promising than those of the strain gauge. The data retrieved from the y-axis laser displacement proved that the cutter did affect the rod during formation. This information re-enforced the assumption that the upstream components of the machine did induce movement into the rod, and thus were needed components in the description of the rod's motion. The plot shown in Figure 3.3

is an example of the mean zero time data drawn from the y-axis laser, where the machine was operating at a speed of 7795 units/min. Failure in the rod occurred at approximately 5.75 seconds into the data record. This was the were the data was trimmed. The trimming location is the point in the data where failure occurs. The data before this point is used, and the data after this point is deleted. Therefore, 16384 points were taken for the FFT which is shown in Figure 3.4. Figure 3.5 is the FFT information of the same data, only it is made-up of 10 averages of 1024 points.

This information would not have led to further testing of this process, if not for another data run that re-enforced the fact that the cutter frequency was showing through in the spectrum. The data corresponding to the data run, Test 2B, also showed the cutter frequency, but in this case it was located at 39.4 Hz. which corresponds to the running speed of 4733 units/min.; which is the operating speed of Test 2B. Figure 3.6 is the FFT with 8 averages of 1024 points.

Axial Velocity

As mentioned earlier, the data from the laser Doppler for axial velocity measurement was collected on a 10 Hz. signal channel; therefore, the Nyquist frequency is 5 Hz. Any frequency above 5 Hz is of no use due to aliasing. This channel had too slow of a response time to be of use in this set of tests. Figure 3.7 shows how the data looks when converted to the frequency spectrum. The slow collection of data minimized the

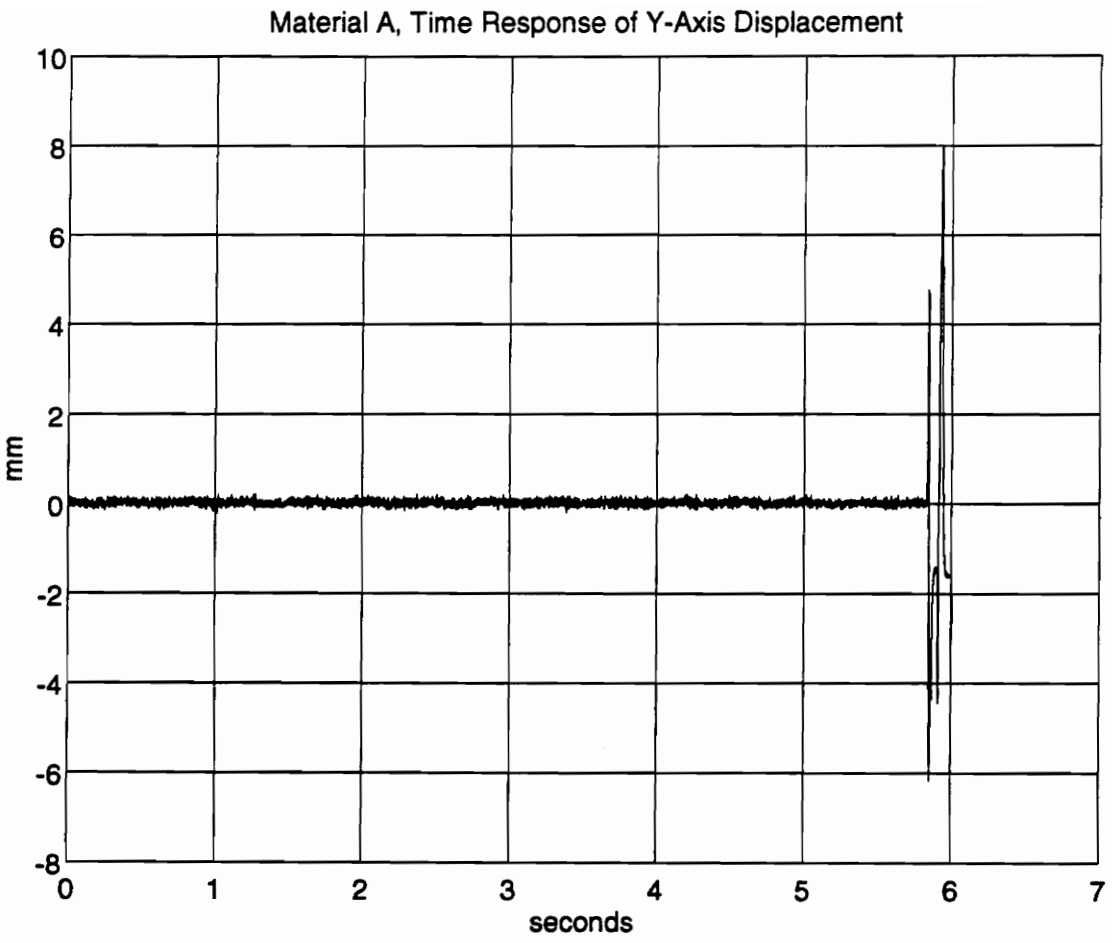

Note: This is a plot of the time signal collected from the y-axis displacement measurement. This was placed in the report to illustrate that the failure in the rod is easy to identify.

Figure 3.3: Time Response of Y-Axis Displacement

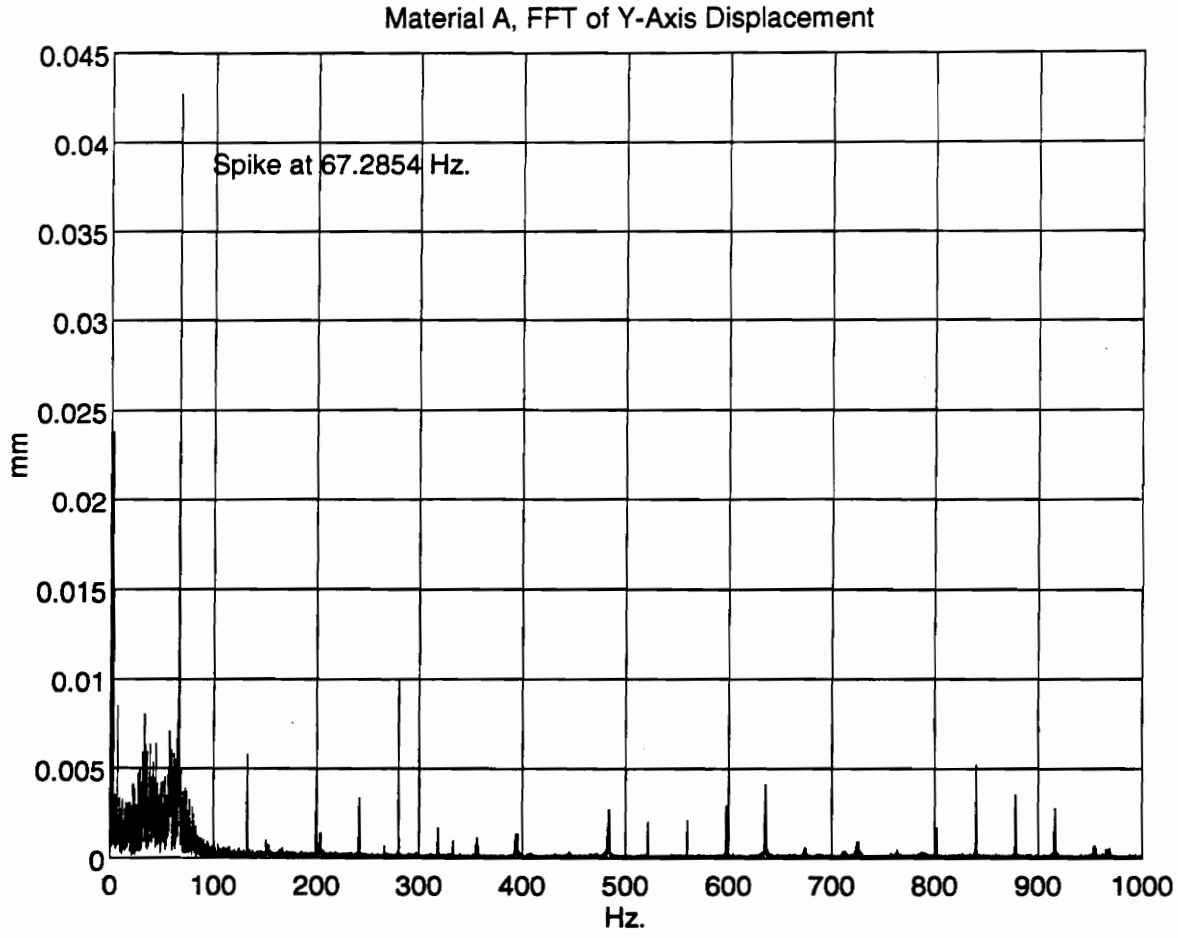

Note: This is a plot of the frequency spectrum from the y-axis displacement measurement. This was placed in the report to illustrate the frequency of 67.2854 Hz. which is approximately the cutter frequency.

Figure 3.4: FFT of the Y-Axis Displacement Measurement

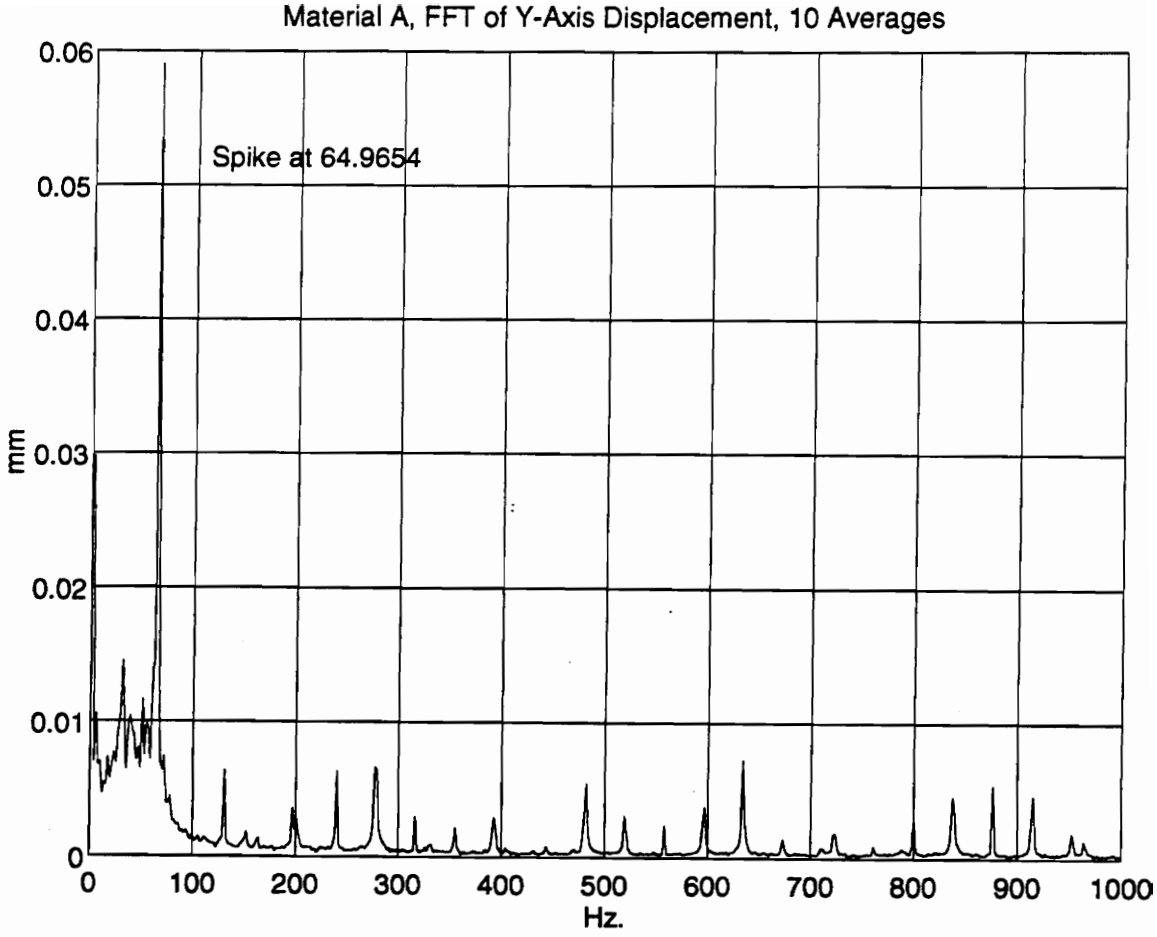

Note: This is a plot of the frequency spectrum from the y-axis displacement measurement. This was placed in the report to illustrate the cutter frequency of 64.9654 Hz. with 10 averages.

Figure 3.5: FFT of the Y-Axis Displacement Measurement, 10 Averages

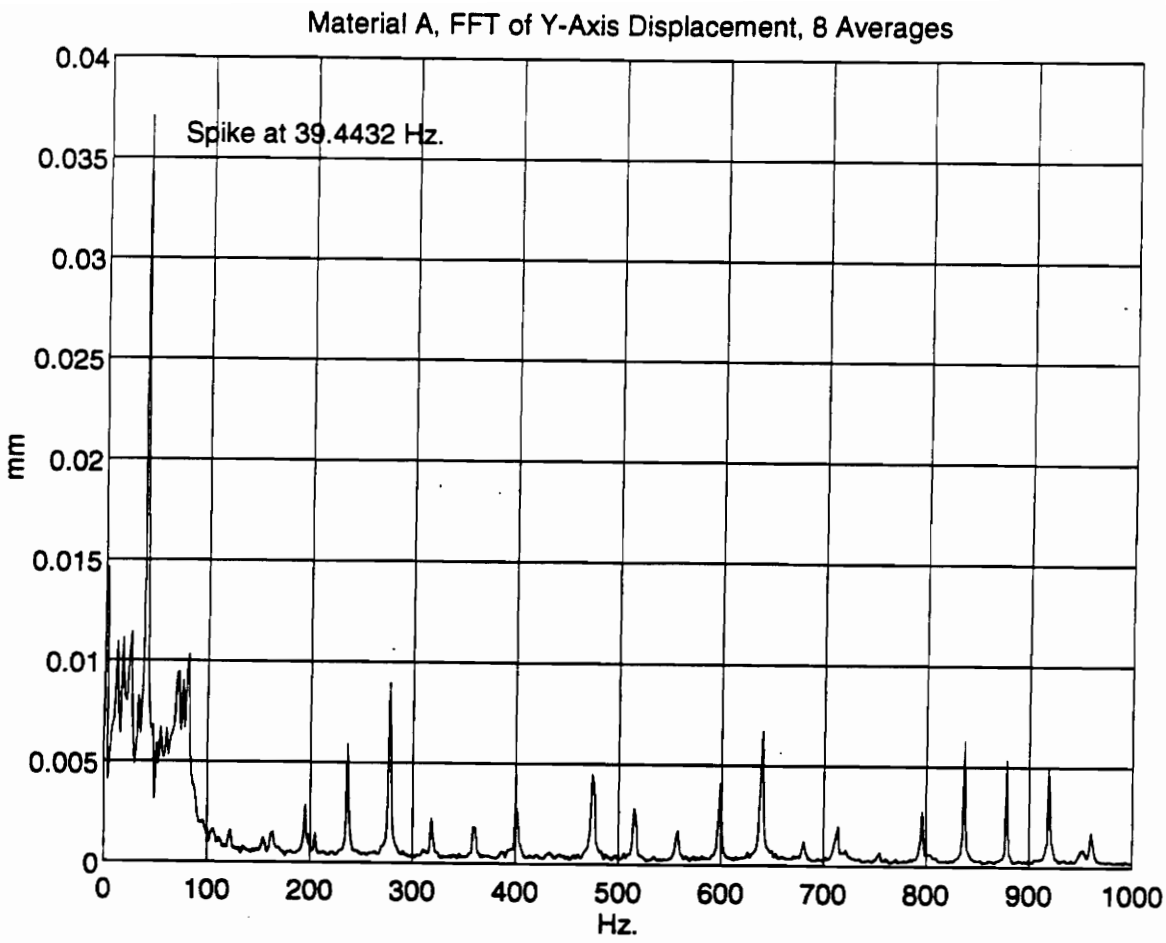

Note: This is a plot of the frequency spectrum from the y-axis displacement measurement. This was placed in the report to illustrate the cutter frequency of 39.4432 Hz. with 8 averages.

Figure 3.5: FFT of the Y-Axis Displacement Measurement, 4733 units/min

resolution of the data, and thus left the data useless for the degree of accuracy and frequency range needed in this experiment.

Draft Pressure Measurement

The draft pressure in the rod shaper had two problems associated with it. The first, which was the problem identified in this experiment, was that the voltage output had no engineering units associated with it. After much searching for the required conversion from voltage to some pressure units, the data was deemed unacceptable for use in this experiment. Without the units for the pressure output, the data could have been composed mainly of noise or vibration of the rod shaper. The second, which was to be discovered after the next set of tests, was that the pressure measurement was not sensitive enough to acquire the frequencies from the downstream devices. The pressure device was originally designed to be a control device that used a long slow trend to control the overall volume of porous fiber used in this process.

Rod Shaper Temperature

The temperature gained from the thermocouple gave information on the normal operating temperature of the rod shaper, but due to the thermal mass of the rod shaper, the frequencies that were needed from this experiment did not materialize. The information needed to predict instantaneous temperature changes from the cutter or other downstream device could not be culled from the thermocouple.

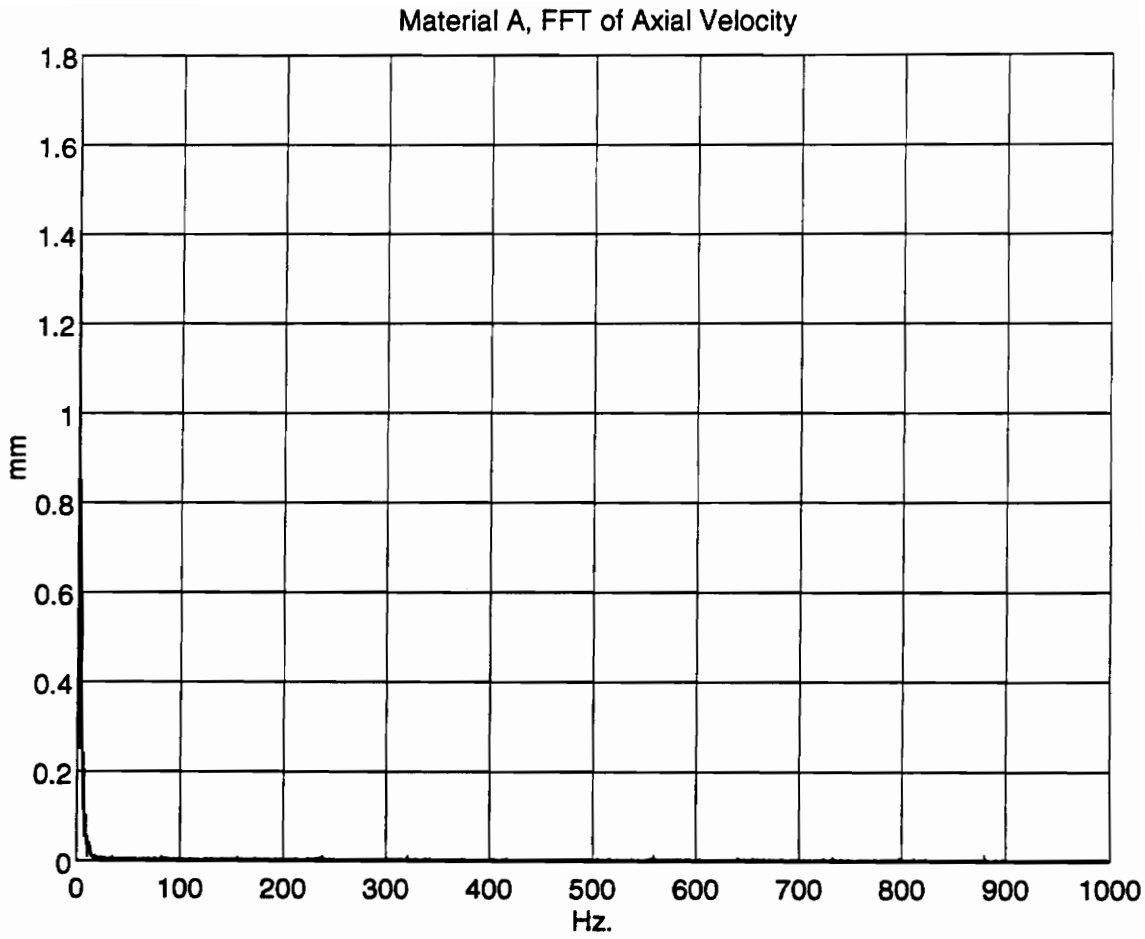

Note: This is a plot of the frequency spectrum from the axial velocity measurement. This was placed in the report to illustrate what the frequency spectrum would look like for data sampled at 10 Hz.

Figure 3.7: FFT of the Axial Velocity Measurement

Test Set Three

Though the data gained from test set two was lacking in many aspects, it did reveal clues as to which direction further experiments should go. The y-axis laser led to the belief that the motion of the rod could be better explained, if an x-axis laser were installed to return the direction of the x-axis. Another lesson learned from the previous test was that the laser Doppler data for the axial velocity measurement needed to be gathered on a faster channel. Also in this set of tests, it was believed that using more than two speeds could be helpful in evaluating whether the changes in machine speeds caused linear or exponential changes in the frequency spectrum. Incorporated in this test array was the use of two materials, Material A and Material B. Though there were two material used, there no depreciable difference in their responses; therefore only Material A will be discussed in detail.

The third set of tests were conducted by two separate parties. One party took data on the experiments mentioned in this report. The second party investigated how much the machine was moving due to normal operating vibrations. This was accomplished through the use of accelerometers placed in several strategic locations on the machine. Excerpts of the data from the second group's results will be included as needed to explain components of the first group's data. It should be mentioned at this point that the data and information presented in this report only represent a fraction of data gathered over the course of this study.

Test set two proved that the displacement in the y-direction was greater than previously thought. The displacement in the y-direction was believed to be a component in the failure of the rod. It was believed that the displacement might increase during fluctuations of the inputs to the rod. It was also thought that the increased displacements would impede the rod's movement into the cutter region and induce failure. If the rod's displacement could be kept to a minimum, then failure might not occur, and the initial disturbance in the rod would be pushed passed the cutter. With the disturbance moved past the cutter, the failure would not occur. With this in mind, a new rod support was designed and built. One test was run with the new rod support in place, and several tests were run with the rod support in place, but not active. When the rod support is not active refers to when the rod support is in place, but not limiting the range of vertical displacement in the rod.

As before, components of the third test array were deemed as unacceptable data, due to various problems associated with it. Similarly to the second test array, the temperature and draft pressure were found to be insufficient, due to the same reasons listed previously.

X-Axis Displacement

From the second test array, it was believed that the x-axis displacement would be useful in developing an understanding as to how the rod behaved. This was implemented in the third test set. Figure 3.8 shows a plot of the typical time data acquired from these

tests, and Figure 3.9 shows the data converted to the frequency domain. One important item to notice is the magnitudes of the displacements shown in Figure 3.9. It can be seen that the displacement is on the order of thousandths of millimeters. The small magnitude would be of little concern if the machine experienced no vibration, but it does. The accelerometer data gathered by the second test group proves that the movement of the x-axis data is not valid. It was found that the laser mounting bracket in the horizontal direction contributes between 10% and 40% of the laser displacement reading. This information combined with the small amplitudes gained from the x-axis testing leads to the belief that the motion of the rod in the horizontal direction is not of significant value when trying to determine the failure modes of the rod.

Y-Axis Displacement

As before, it was known that the y-axis displacement was giving information about the cutter's affect on the rod; however, since the second test set did not incorporate accelerometer data, it was not known if the data was valid. Fortunately, unlike the x-axis data, the laser mounting bracket only accounted for approximately 10% of the total displacement measured. Since the displacements associated with the y-axis displacement was large relative to the x-axis displacement, this data was deemed as acceptable. With this in mind, there are two key ideas to be gleaned from another set of tests dealing with the y-axis displacement. The first is a variation of running speeds, and in this case the machine was run at 5000, 7000, and 8000 units/min. The second idea was to evaluate

how exchanging the original rod support for a modified rod support would effect how the rod's displacements.

Figures 3.10-3.12 show the frequency spectrum of 8000, 7000, and 5000 units/min respectively. Earlier it was believed that knowing how the displacements varied with speed could help to determine if the displacements changed linearly or exponentially, unfortunately due to time constraints and data storage constraints there was not enough speeds tested to determine the character of the displacements. From the three speeds that were run, the displacements seem to be independent of speed. The 5000 and 8000 units/min. case had slightly higher displacements than did the 7000 units/min case. The conclusion to be drawn from this is not clear. With more data points to evaluate, the curve that explains the operating conditions of the machine might be mapped out, but in this case that data is currently unavailable. One detail to make note of in Figures 3.10-3.12 is the energy distribution in the spectrum from 0 to 100 Hz. This smear in the spectrum is the same for all cases, both those shown in this report and those that are not. The smear has a distinct shape and is independent of speed. This is believed to be due to interaction between the rod and the rod support. The second data group performed hit tests on the rod support and found that its resonance frequency was in the lower end of the spectrum. This has a great impact on how the rod might behave if the vibration of the rod support happens to lineup with or correspond closely to the cutter frequency. This will act to amplify the rod's displacement, which in turn could lead to failure of the rod

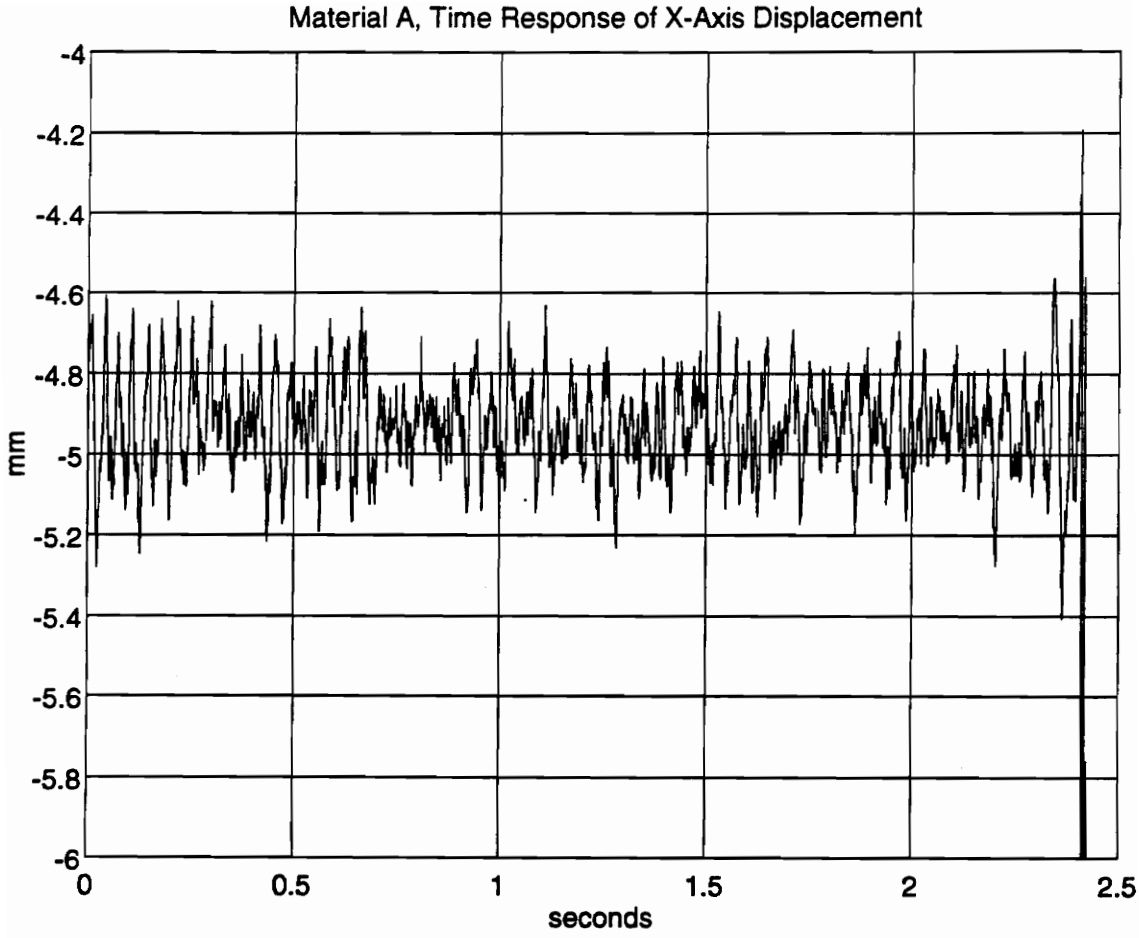

Note: This is a plot of the time signal from the x-axis displacement measurement. This was placed in the report to illustrate what the typical data from this signal looked like.

Figure 3.8: Time Response of X-Axis Displacement

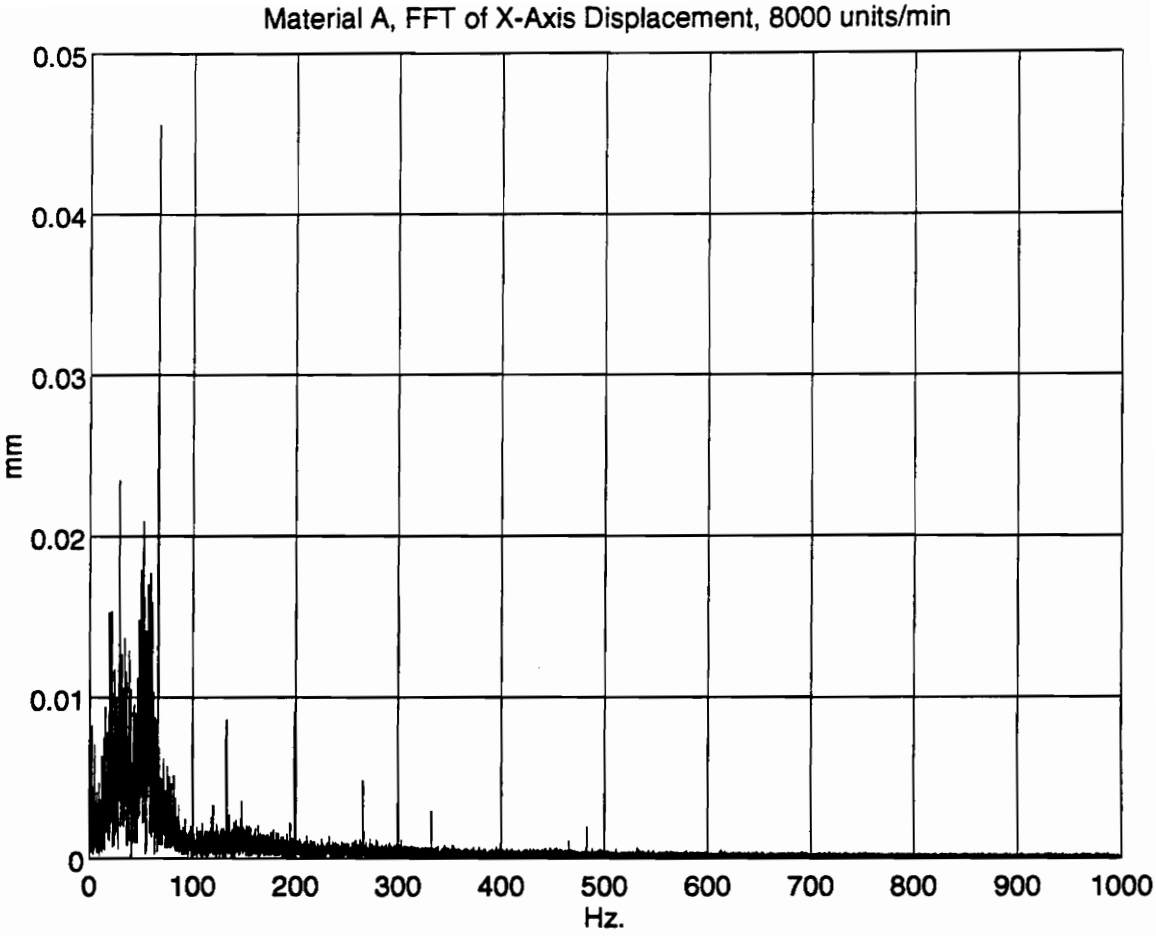

Note: This is a plot of the frequency spectrum from the x-axis displacement measurement. This was placed in the report to illustrate the small magnitudes of the spectral lines.

Figure 3.9: FFT of the X-Axis Displacement Measurement

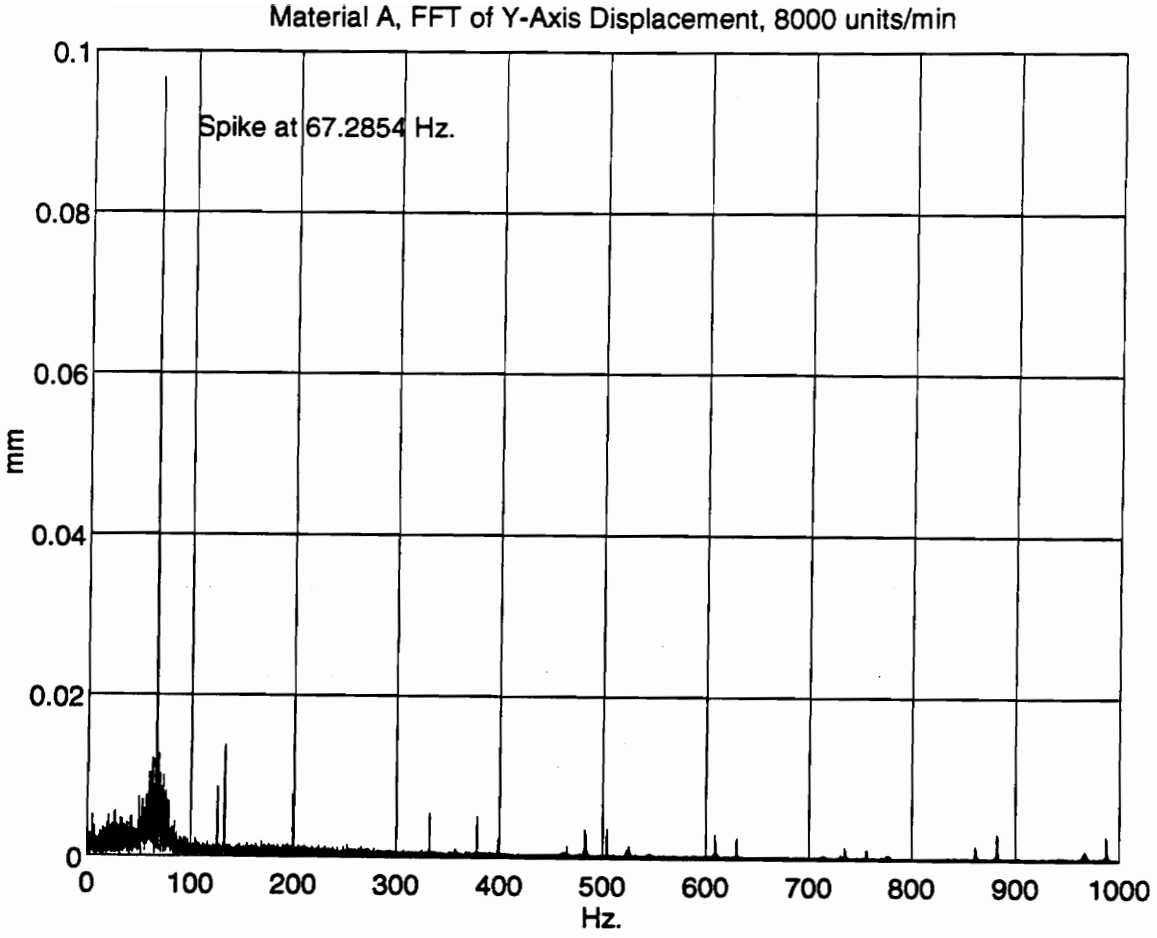

Note: This is a plot of the frequency spectrum from the y-axis displacement measurement. This was placed in the report to illustrate the cutter frequency of 67.2854 Hz. at 8000 units/min.

Figure 3.10: FFT of the Y-Axis Displacement Measurement, 8000 units/min

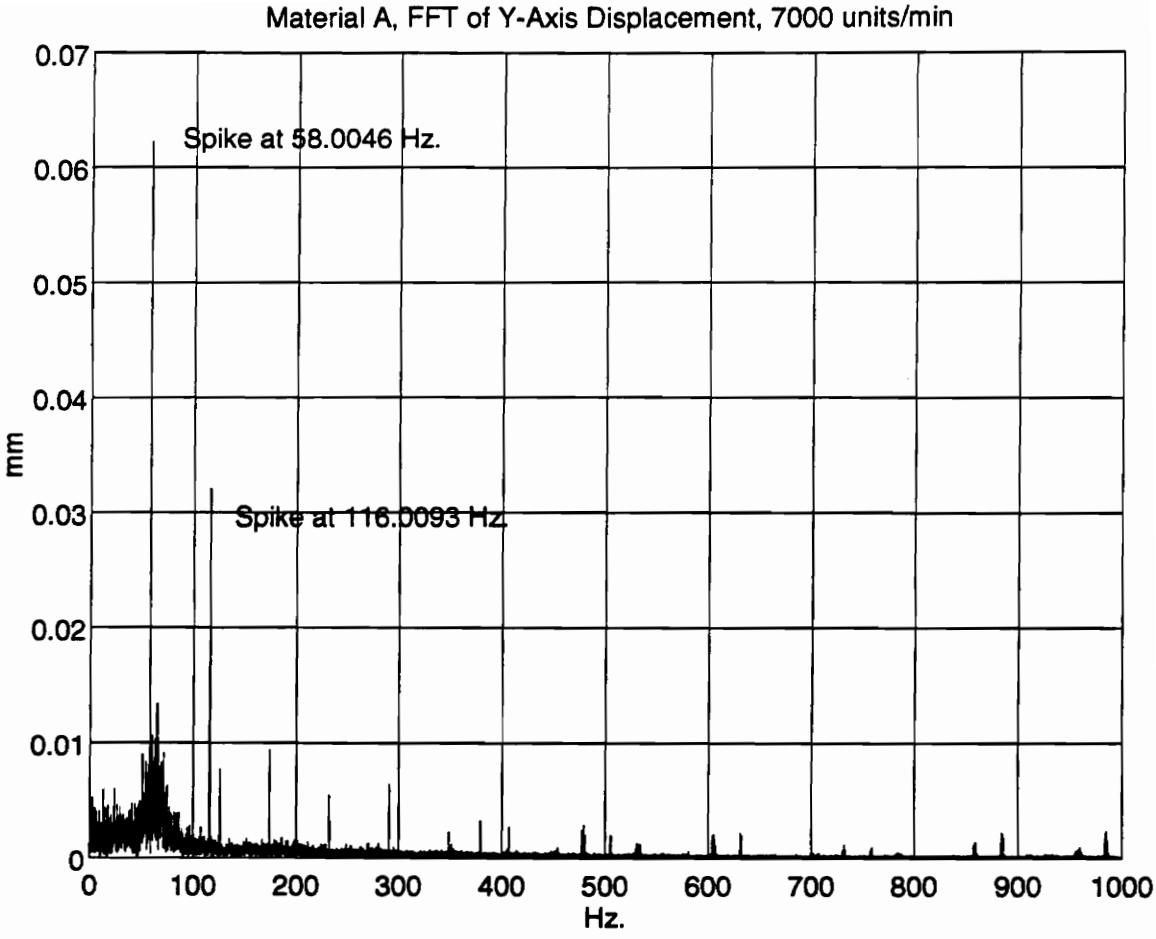

Note: This is a plot of the frequency spectrum from the y-axis displacement measurement. This was placed in the report to illustrate the cutter frequency of 58.0046 Hz. (harmonic at 116 Hz.) at 7000 units/min.

Figure 3.11: FFT of the Y-Axis Displacement Measurement, 7000 units/min

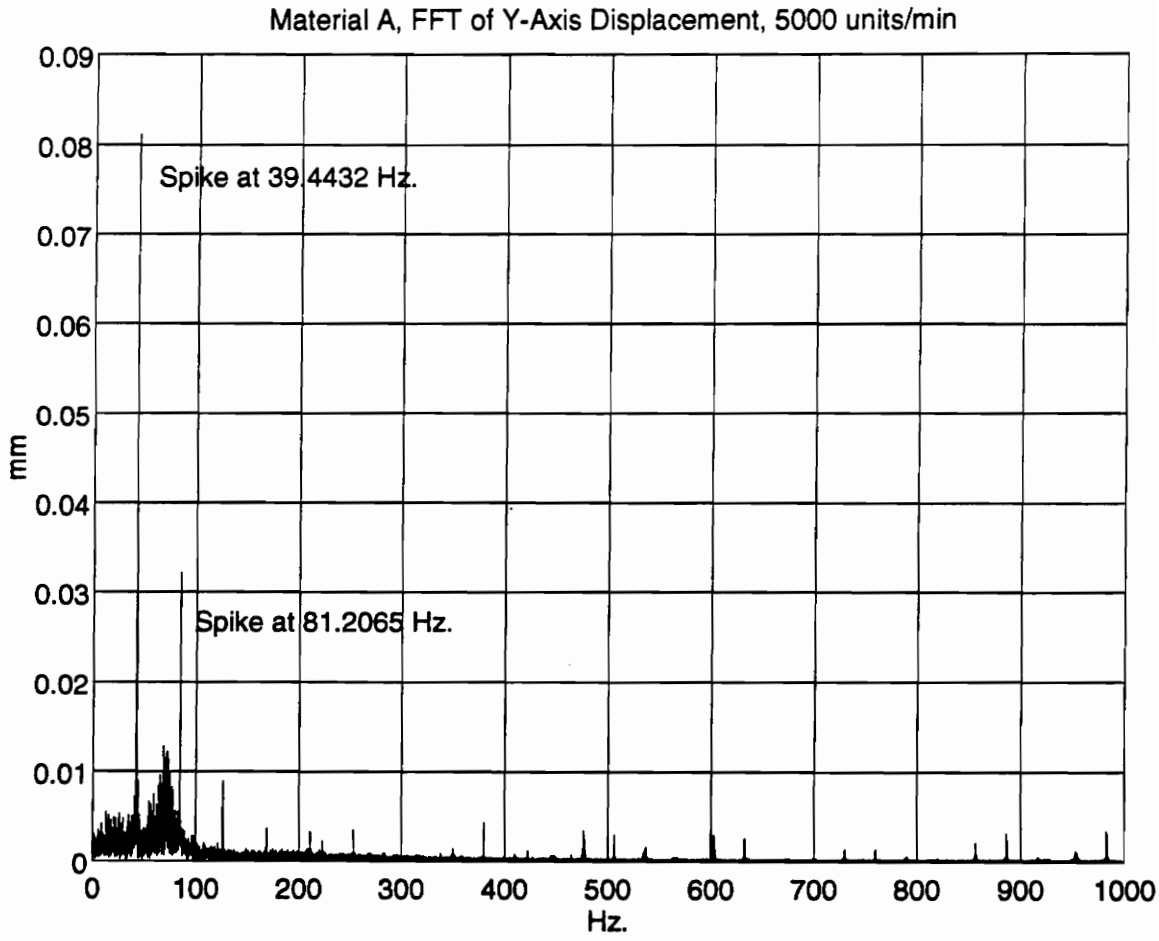

Note: This is a plot of the frequency spectrum from the y-axis displacement measurement. This was placed in the report to illustrate the cutter frequency of 39.4432 Hz. (harmonic at 81 Hz.) at 5000 units/min.

Figure 3.12: FFT of the Y-Axis Displacement Measurement, 5000 units/min

itself. This is an important piece of data. When the new rod support was installed, the energy at the frequency that represents the rod support shifts up in the spectrum.

Figure 3.13 shows the frequency spectrum of the rod when the new rod support is actively used. The new rod support is shown in Figure 3.14. It can be seen that the energy dispersion maintains the same general shape, but in this case it is moved past 100 Hz. Another detail that should be noticed is how the displacement is significantly less than the case for the original rod support at the cutter frequency. This may be due to the fact that the frequency for the new rod support is above the cutter frequency. By separating the cutter energy from the rod support energy, the displacement drops and the rod has considerably less movement. Another spike is also seen now, but is around 120 Hz. The cause of this input is not known currently, but its increase in magnitude is probably due to the movement of the energy from the rod support.

This movement in the rod support frequency is not due to the active use of the new rod support. Figure 3.15 shows that when the new rod support is in place, but not actively used, the spectrum changes and the displacement drops in magnitude. This means that changing the rod support, so that its resonance frequencies do not fall near other input frequencies, should lower the deflections of the rod. Figures 3.16 and 3.17 also support this theory. They are for the new rod support, not actively used, at 7000 and 5000 units/min. respectively. The magnitude of the cutter frequency is lessened with the new rod support and this should lessen the displacement of the rod.

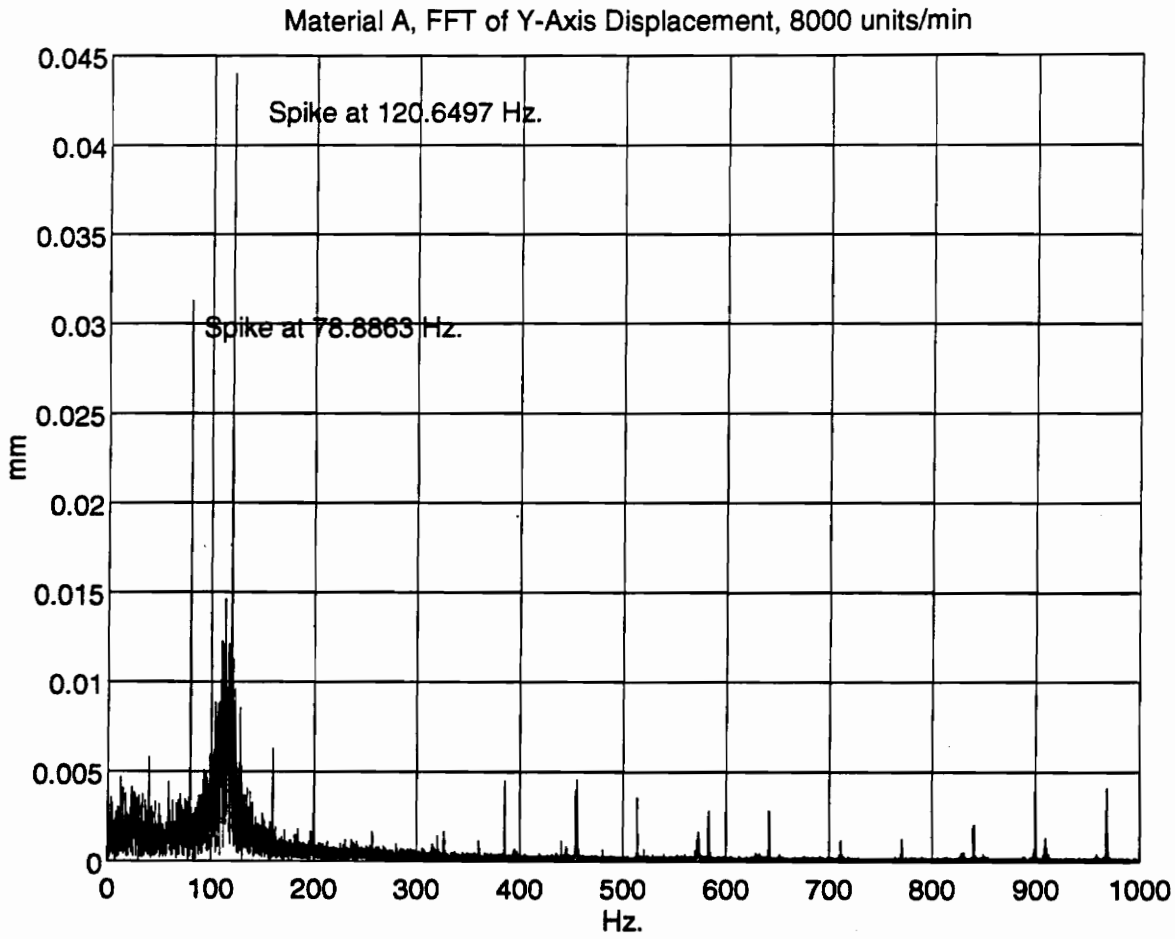

Note: This is a plot of the frequency spectrum from the y-axis displacement measurement. This was placed in the report to illustrate the effects the active rod support on the magnitudes of the spectral lines.

Figure 3.13: FFT of Y-Axis Displacement With Active Rod Support

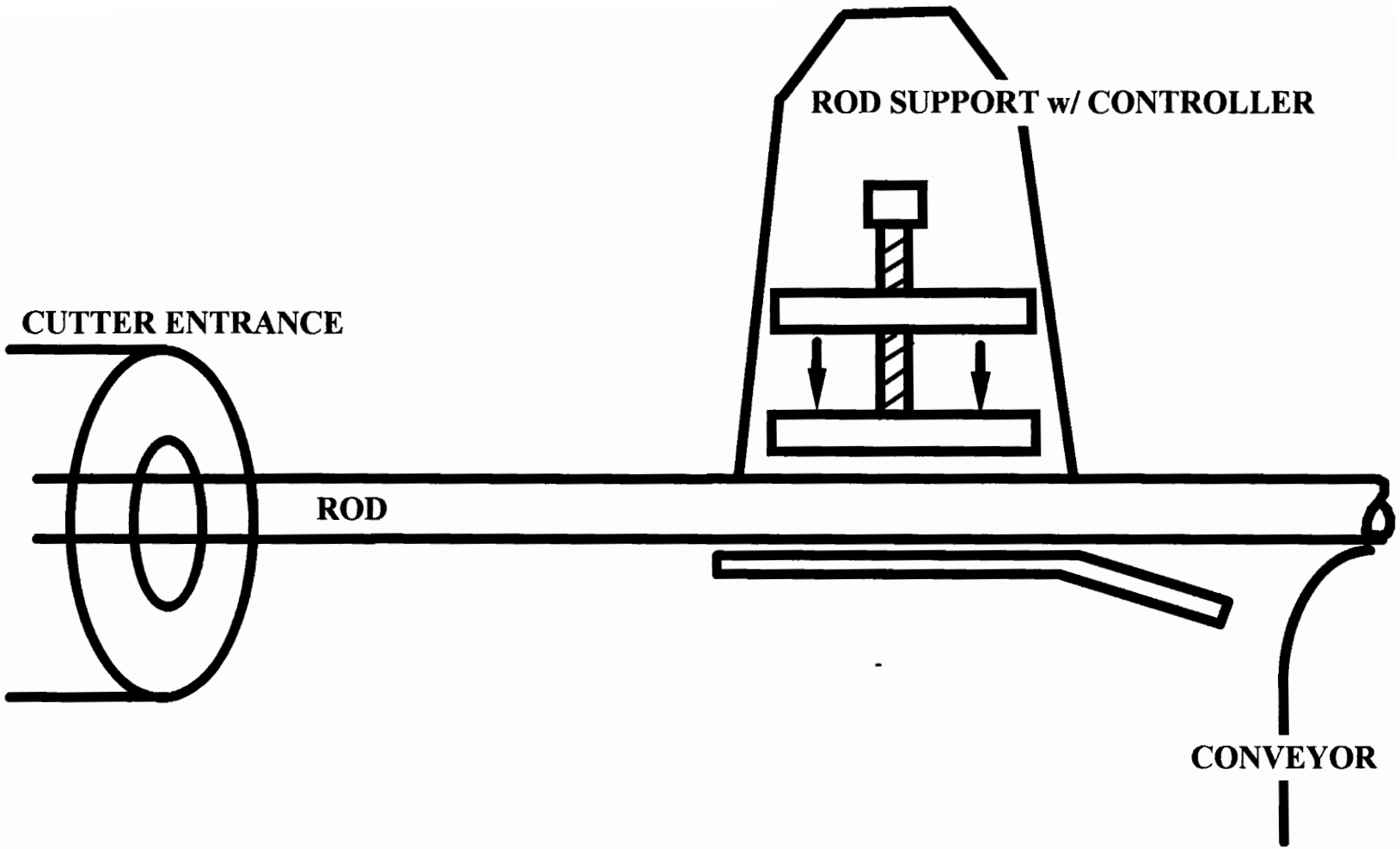

Figure 3.14: New Rod Support Region

Axial Velocity

The axial velocity information from this round of tests did little to improve the understanding of the rod motion. The axial velocity shown in Figure 3.18 shows a very clean spectrum. This is typical of the data obtained from the velocity measurement. However, the time response shown in Figure 3.19, is representative of data that has been clipped. This means the range on the velocity was larger than the range the data could be collected in. This infers that the magnitude of the data may not be of any use; however, the frequency information may be.

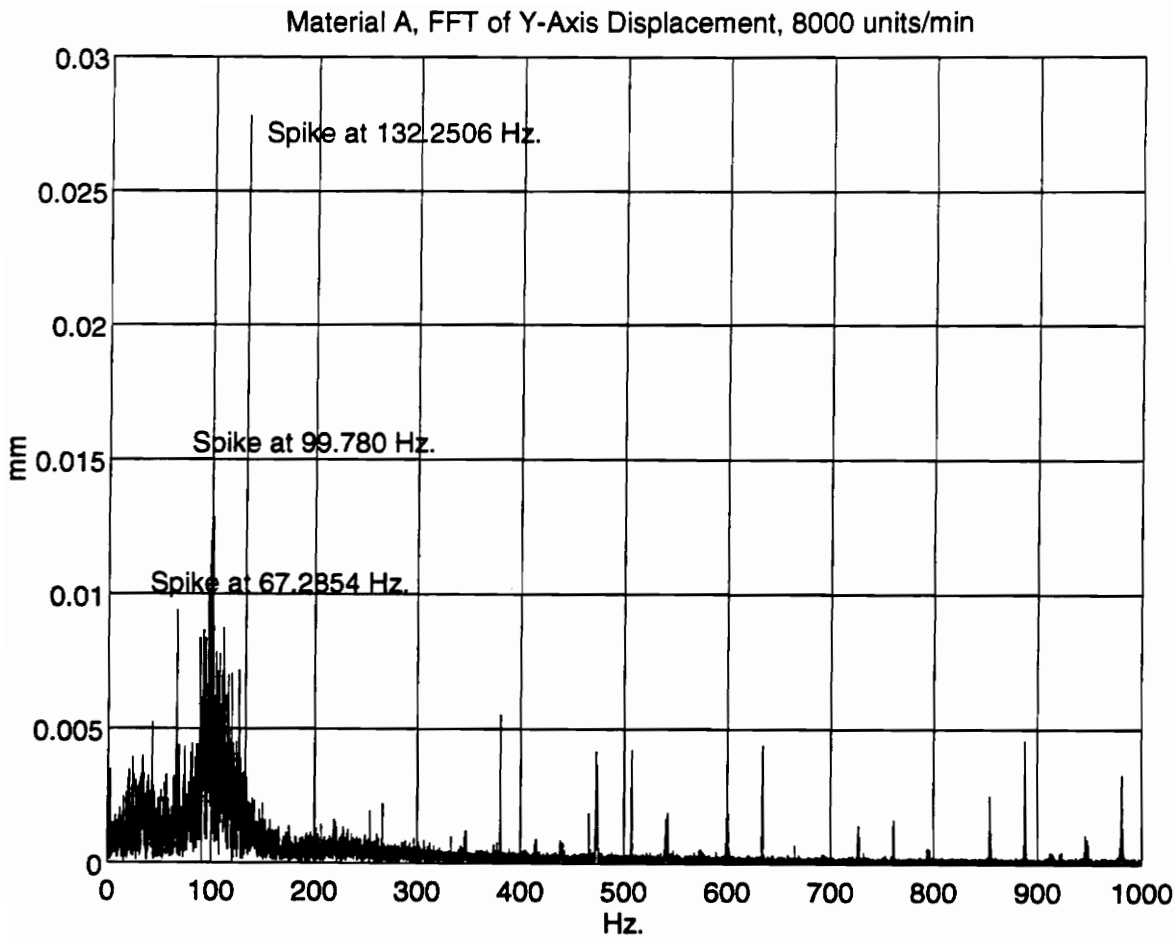

Note: This is a plot of the frequency spectrum from the y-axis displacement measurement. This was placed in the report to illustrate the effects of the new rod support when not active, 8000 units/min.

Figure 3.15: FFT of Y-Axis Displacement With New Rod Support, Not Active

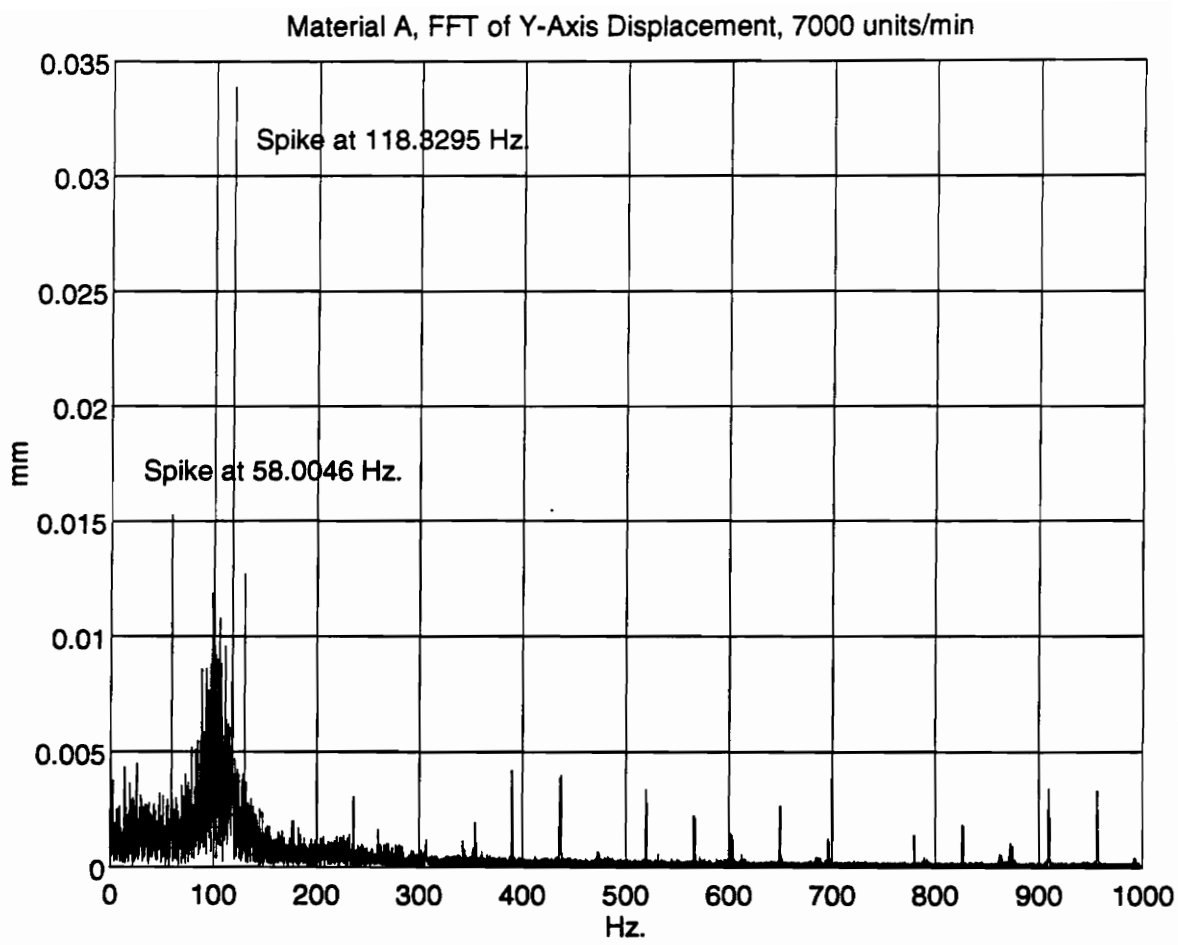

Note: This is a plot of the frequency spectrum from the y-axis displacement measurement. This was placed in the report to illustrate the effects of the new rod support when not active, 7000 units/min.

Figure 3.16: FFT of Y-Axis Displacement With New Rod Support, Not Active

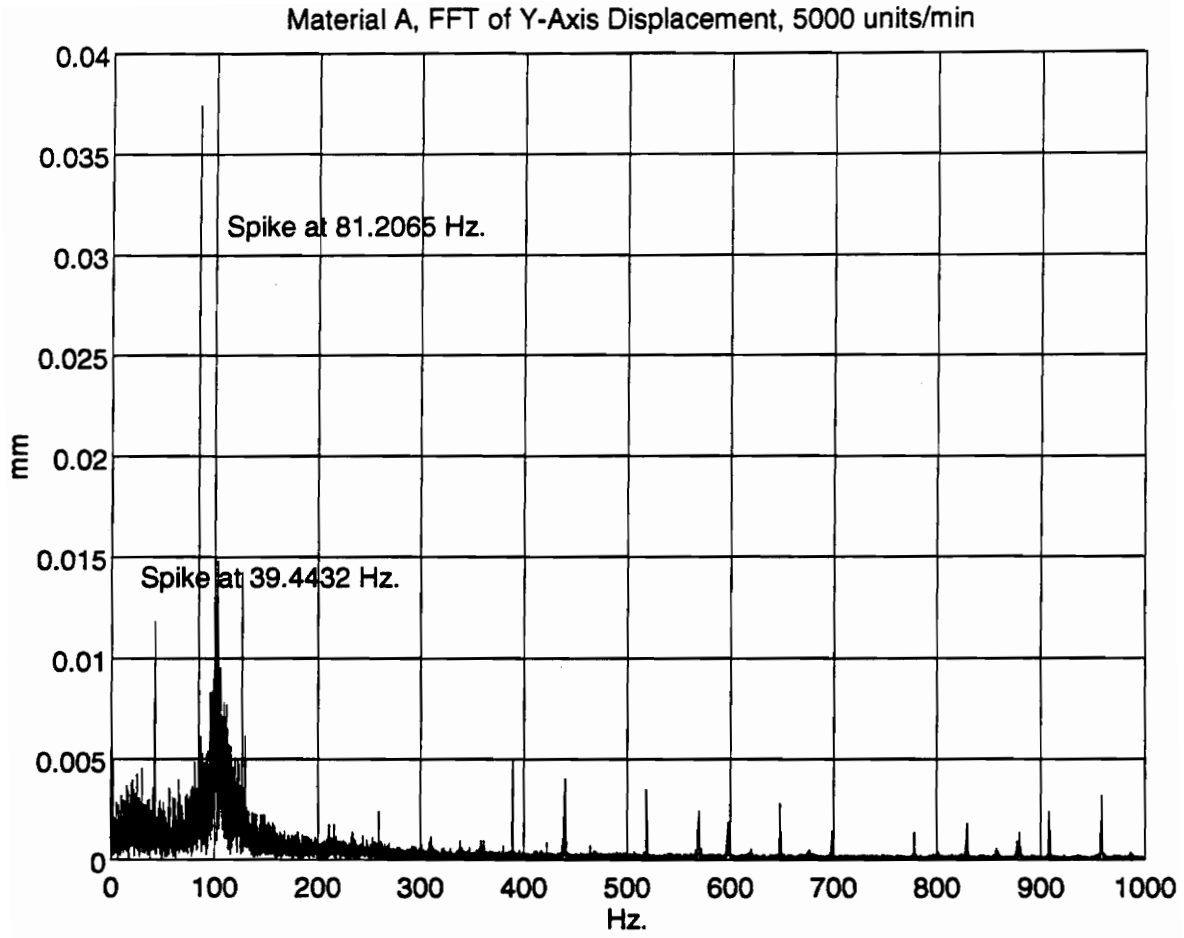

Note: This is a plot of the frequency spectrum from the y-axis displacement measurement. This was placed in the report to illustrate the effects of the new rod support when not active, 5000 units/min.

Figure 3.17: FFT of Y-Axis Displacement With New Rod Support, Not Active

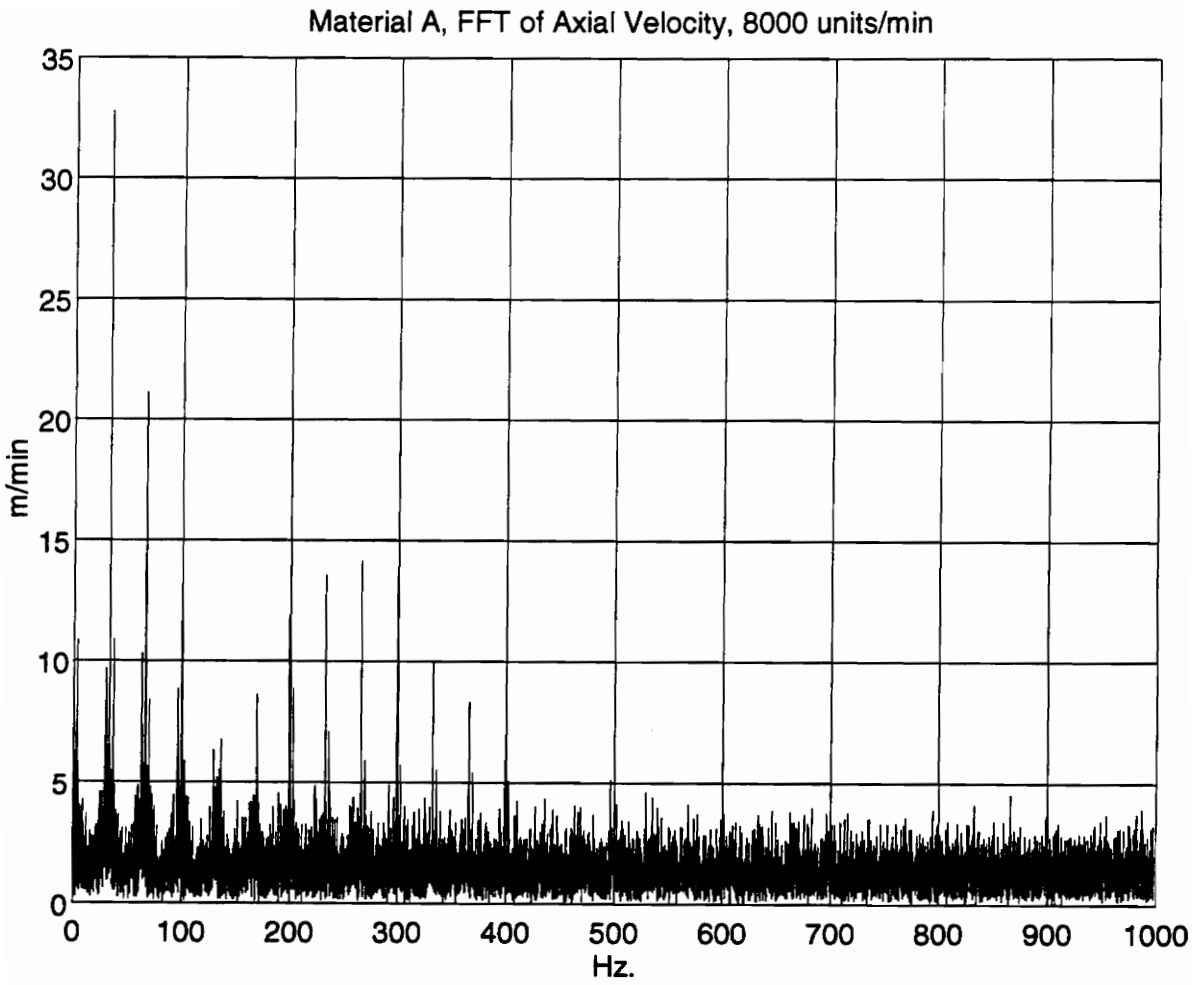

Note: This is a plot of the frequency spectrum from the axial velocity measurement. This was placed in the report to illustrate that a clipped signal will not yield useful information.

Figure 3.18: FFT of Axial Velocity, 8000 units/min

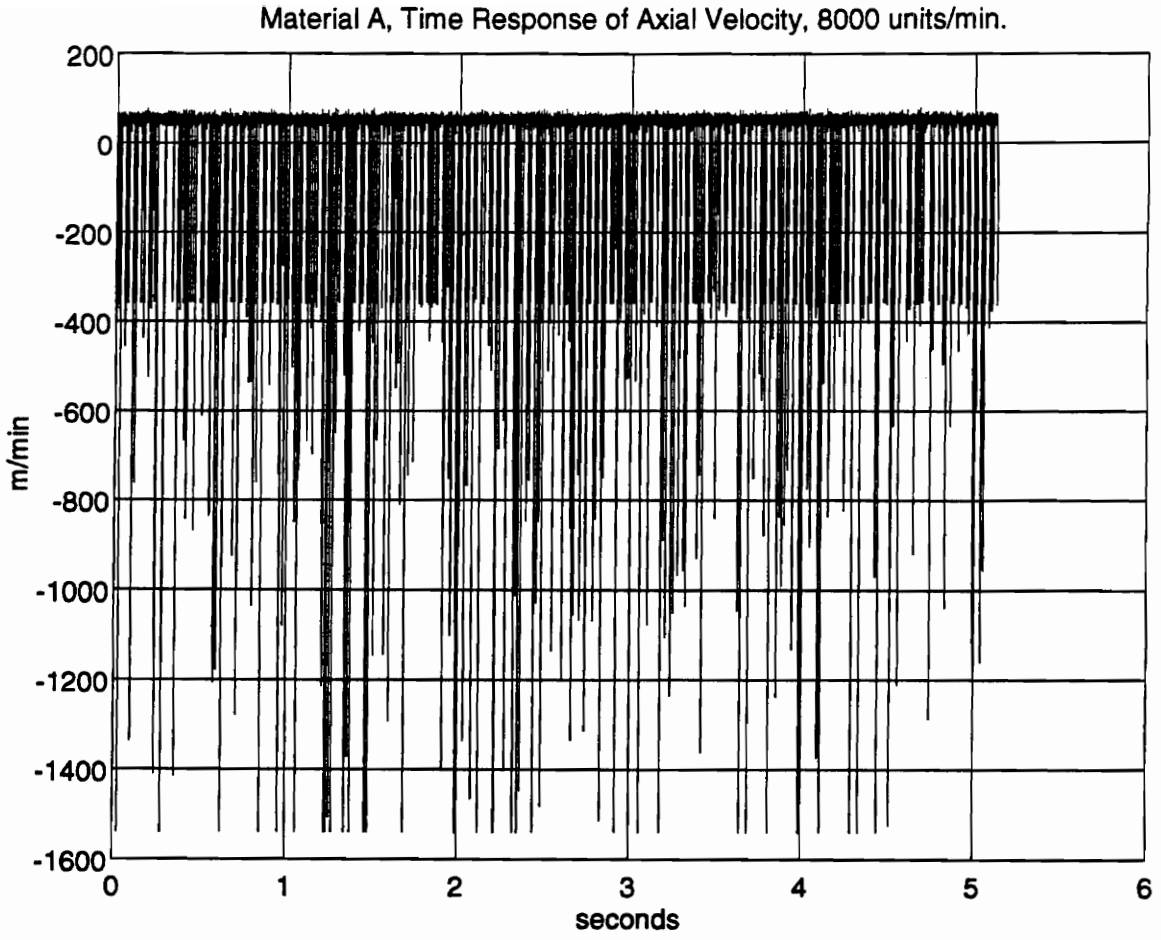

Note: This is a plot of the time signal the axial velocity measurement. This was placed in the report to illustrate how a clipped signal in the time domain will look.

Figure 3.19: Time Response of Axial Velocity, 8000 units/min

IV. REVISED TEST PROCEDURE

Due to logistical problems, many of the tests performed in this research were lacking. This unfortunately led to a weak conclusion of the results. Upon review of the tests and procedures, it was believed that an improved conclusion could be attained by developing a more precise test procedure. The following procedure offers an alternative to the earlier tests, and if implemented, it is believed that this new approach will return a better solution to the rod formation problem.

General Procedure

The results from the earlier tests revealed that the rod shaper region is a difficult component to attain measurements from. Knowing this it would be prudent to bypass testing in this region and use those resources to better examine the rod support and cutter regions.

In the rod support region, X and Y axis testing would be beneficial to the study of the rod's motion. This data needs to be collected simultaneously with accelerometer measurements. The accelerometers need to be mounted on or near both of the displacement lasers and also on the rod support itself. This will allow for cross-referencing of the data. Also in this region, the axial velocity needs to be measured while the other data is being collected. This will also allow for future simultaneous evaluation.

In the area of the cutter, the rod pulses need to be collected so that the data from the displacement measurements can be aligned with the cutting motion. Another component to consider in this region is the use of high speed video. Video of the actual cut would allow the rod to be visually inspected during each cut to determine if there are any visible deflections in the rod during the cutting process.

Detailed Evaluation

If the data is assumed to be stationary, the first element to consider in this section is the use of averaging to improve the statistical significance of the data. The data time records need to be broken into 2^n units, where n is an integer. After the files have been broken up, a FFT should be performed on each of the components. Then the FFT information should be summed and divided by the number of individual files. This will lower the chances that a single abnormality in one of the records will lead to erroneous interpretation.

In the purposed setup, the rod support region will offer the largest block of data. The accelerometer data collected from the displacement lasers and the rod support need to be integrated twice with respect to time to place it the same domain as the laser displacement data. The axial velocity should also be integrated, but only once. Integrating the accelerometer data is preferred to differentiating the displacement and velocity data. Differentiating will lead to the amplification of the random noise always found in the data. From this point, all of the data is in terms of displacement and this

should also be averaged. With all of this data in place and averaged, the rod pulse signal can be incorporated into the data. This meshing of the data will allow the cutter motion to be aligned with the data from lasers and accelerometers.

The displacement data from the accelerometers offers a way of determining how much the displacement lasers are actually moving with respect both to the earth and to the machine. This will allow the absolute displacement of the rod to be determined and thus can be aligned with the cutter blade.

Each set of data should be autocorrelated to determine which spectral lines in the FFT are random. The autocorrelation function for a random process x(t) is defined to be the average of the product of $x(t)x(t+\tau)$. The data is collected at time t and then again at time $t+\tau$. The product of the two are then averaged for the ensemble, E[of $x(t)x(t+\tau)$]. If the data collected is stationary, independent in time, the value of E[of $x(t)x(t+\tau)$] will be independent of absolute time t and will depend only on the time separation of the two records τ. Therefore the autocorrelation function for x(t), $R_x(\tau)$ is defined as follows.

$$R_x(\tau) = f(\tau) = E\left[x(t)x(t+\tau)\right]$$

A property of $R_x(\tau)$ is that if x(t) is stationary then the mean and standard deviation of the will be independent of time therefore:

$$E\left[x(t)\right] = E\left[x(t+\tau)\right] = m$$

and the deviation, σ, of both t and $t+\tau$ are equal. The correlation coefficient that relates the record is defined to be:

$$\rho = \frac{R_x(\tau) - m^2}{\sigma^2}$$

When the value of $\tau \to \infty$ the value of $R_x(\tau)$ approaches m^2. This means that a random process will have a correlation coefficient of $\rho = 0$. In simple terms this means that any data that is random, including random phase in periodic data, will go to zero when the autocorrelation is performed.

Another calculation that needs to be performed is a cross-correlation. This is similar to the autocorrelation, only it correlates two stationary random processes. These processes can be represented as two functions in time, x(t) and y(t). As before, the records are collected at time t and at time $t + \tau$. If this is the case, then it follows that the cross-correlation coefficients are as follows:

$$R_{xy}(\tau) = E[x(t)x(t+\tau)]$$

$$R_{yx}(\tau) = E[y(t)y(t+\tau)]$$

Since the processes are stationary, it follows that:

$$R_{xy}(\tau) = E[x(t-\tau)y(t)] = R_{yx}(-\tau)$$

$$R_{yx}(\tau) = E[y(t-\tau)x(t)] = R_{xy}(-\tau)$$

Each cross-correlation function can be expressed in terms of the corresponding normalized ρ, which yields:

$$R_{xy}(\tau) = \sigma_x \sigma_{yx} \rho_{xy}(\tau) + m_x m_y$$

$$R_{yx}(\tau) = \sigma_y \sigma_{yx} \rho_{yx}(\tau) + m_y m_x$$

As in the autocorrelation case, as $\tau \to \infty$ then it follows that:

$$R_{xy}(\tau \to \infty) \to m_x m_y$$

$$R_{yx}(\tau \to \infty) \to m_y m_x$$

This means that the value of ρ approaches zero for random data; therefore, cross-correlating the data will link the two data sets and return which components in the data are dependent on each other.

Another concern to focus on is the way that the accelerometer data and the displacement data are compared. The real components from the FFT represent the magnitude of the data and the imaginary components represent the phase relation of the data. This means that the phase information from the integrated accelerometer data and the laser data must be compared. When the two are out-of-phase this means that they are moving in opposite directions. And when they are in-phase this means that the accelerometer and the lasers are moving together in the same direction. This will determine their relative and absolute motions.

Interpretation

Once the above procedure has been performed, the next step is to evaluate exactly what the data means. Each spectral line should examined and if possible identified. The

upper frequencies may be harmonics of some lower frequencies. The spectral lines may be small in their magnitude but may offer insight as to the actual physics of the problem.

When all of the data is averaged, correlated, and labeled then and only then can a solid explanation of the dynamics of the machine and the rod may be expressed. This procedure is the correct approach to the problem of signal processing. The conclusions and recommendations made in this report represent a deduction of certain clues and is not a detailed mathematics approach due to the lack of certain required information.

V. CONCLUSIONS AND RECOMMENDATIONS

Conclusions

The information gained from these sets of tests seemed in many instances to lead to useless information; however, this is not an entirely true statement. The information leads to questions that may in the future be beneficial to the researchers who are trying to improve this rod making process.

The high speed video used in the early study of this problem proved crucial in the evaluation of what direction the tests should take. The video proved that the rod did move more than the eye could perceive. The displacements in the y-axis direction were large enough just before failure to show that understanding and controlling its displacement would be useful in improving the performance of the machine.

The y-axis displacement data gave the best indications of how the rod behaved. Since the magnitude of the rod's displacement did not vary greatly with speed in the spectral plots, the data showed that the deflection of the rod was not strongly machine speed dependent,. This was a surprising result. Granted more data at many different speeds would be helpful in laying out a set of operating curves, which would be useful to operation, but from the three speeds evaluated the amplitudes of the displacements did not vary significantly from one speed to the next.

Also gained from y-axis displacement was an understanding that the rod support did vibrate in a range which might act to magnify the displacements of the rod. From the

data gathered from both the old and new rod support, it is believed that adjusting the rod support would improve the performance of the machine.

The axial velocity did not return the degree of detailed information that was originally hoped would come from it. The axial velocity did not return the inputs of the cutter and the other inputs from the machine. This is do to several problems. The second test set information was of no use since it was collected on a slow channel. The third test set data was clipped which gave no useful information. The last problem was that even if acceptable data was gathered for the component of the test array, it is questionable if the information gathered would be useful for gaining an understanding about any input other than the cutter.

The x-axis information was helpful, even though it was deemed as unacceptable. It did reveal that the displacements in the x direction were small. By knowing the x displacements were small in comparison to the y direction, it can be assumed that the dominating movement is in y-axis direction. Future testing should focus on the y-axis displacements.

The three other components discussed; temperature, draft pressure, and axial force, were good approaches on how to find inputs on the rod. However they proved impractical in their implementation. The response time and the sensitivity required for these measurements would require a large financial investment to purchase the testing equipment needed and would probably not lead to a large enough financial return for the investment required.

Recommendations

The y-axis rod displacement does have an input from other components of the machine. One of the largest inputs comes from the cutter region. To lessen the input from the cutter, it would be beneficial to implement a new rod support that acted to dampen this effect. This solution would be two fold in its return to the overall operation of the machine. The current rod support has an input on the rod that acts to increase the deflection in the vertical direction. By changing to a rod support that would actively damp the cutter input, the new rod support's input to the rod might be moved out of the frequency range that causes problems in performance.

The machine in this study is pushing the upper limit of its capacity to run. The problems with production stops will not be corrected with one sweeping reform or change to the machine. The problem is that all of the small problems associated with these high speeds have bottlenecked, and when one is removed, another rushes in to take its place. To improve the overall performance of the machine will require that the components that are in direct contact with the rod be evaluated to determine if their resonance frequencies fall within the range with large inputs such as those from the cutter. Replacing the rod support will probably, over an extended operating period, lessen machine stops. Evaluating the components in the cutter region to determine if their motion acts to retard the speed of the rod would probably bear fruit in the form of a redesign.

REFERENCES

Bechwith and Marangoni, 1990, Mechanical Measurements, 4th ed., Addison-Wesley Publishing Company, pp. 702-713.

Newland, D.E., 1993, An Introduction to Random Vibrations, Spectral & Wavelet Analysis, 3rd ed., Longman Scientific and Technical, pp. 113-224.

Rao, S.S., 1990, Mechanical Vibrations, 2nd ed., Addison-Wesley Publishing Company, pp. 37-45.

VITA

The author, Shannon Thomas Stewart, was born in Vicenza, Italy on January 9, 1972. He grew-up on a farm in southwest Virginia. He lived there until he came to Virginia Tech in 1990 were he then became a mechanical engineer. Then in May of 1994 he began his master's degree. His future plans are to return to southwest Virginia and to venture into some yet unknown field.